

INVESTIGATION OF INTERACTION PARTNERS OF NLRP13

by

Hilal Ok

B.S., Molecular Biology and Genetics, Izmir Institute of Technology, 2018

Submitted to the Institute for Graduate Studies in
Science and Engineering in partial fulfillment of
the requirements for the degree of
Master of Science

Graduate Program in Molecular Biology and Genetics
Boğaziçi University

2022

ACKNOWLEDGEMENTS

Above all, I would like to express my gratitude to my supervisor Prof. Dr. Nesrin Özören who gave me the opportunity to work in her studies taking me far beyond where I am, enabled me to develop both scientifically and socially, and provided valuable guidance during the years we worked together. I would like to extend my special thanks to my defense committee members Assoc. Prof. Umut Şahin and Assoc. Prof. Duygu Sağ for giving their valuable time to evaluate my thesis and for offering me their precious comments guiding my perspective in this study.

Moreover, I would like to show my appreciation to Prof. Dr. Gizem Dinler Doğanay and her student Baran Dingiloğlu, M.Sc., from Istanbul Technical University, and Prof. Dr. Ferruh Özcan and his student Mehmet Soner Türküner, M.Sc., from Gebze Technical University for their great support about sample preparation procedure for mass spectrometry, mass spectrometry process and data analysis.

My eternal gratitude to dear most spectacular lab mates ever İlke Süder, M.Sc., Hafize Özen Kaya, M.Sc., Davod Khalafkhany, M.Sc., Efe Elbeyli, M.Sc., Sevgi Çıracı, M.Sc., Elif Öykü Çakır, M.Sc., and İrem Ceren, B.Sc.. They provided me with many unforgettable experiences that will allow me to stand out in many areas of life with their scientific guidance and exclusive personalities. My sincere thanks to Davod in particular and İlke and Özen for being patient with me even with my foolish questions and being my concealed advisors all along the line. Working with the other members of the NLRP13 team, Sevgi and Öykü, was a privilege. I look ahead to reliving our full-of-fun dates. Regardless of day or night, both our classiness and goofiness when we were together was immense. I am grateful to all these precious people for their time to me and for their emotional support and encouragement. They made my life more bearable in every sense with their wonderful sense of humor.

Additionally, I would like to thank to Sütlü Lab, SUMO Lab, and GenReg Lab for providing the needed materials and equipment used in this study and to many

people in the department for being helpful and kind.

Special thanks to my dear friend Dilanur Meti, whom I consider as my sister, who has been in my life for more than fifteen years, for always being there for me and being proud of me. I am proud to have you.

My most special thanks, which will never be enough no matter how much I would say, to my loving and self-sacrificing mom and dad, Hanife and Üzeyir Ok, and my little prince Ahmet Berk Ok for their endless patience, unconditional trust and pure love along this bumpy road - without them nothing would be possible.

ABSTRACT

INVESTIGATION OF INTERACTION PARTNERS OF NLRP13

NOD-like receptors (NLRs) are the cytoplasmic members of pattern recognition receptor family, broadly with functions in inflammasome formation, signal transduction, transcription activation, cell death, reproduction, and embryonic development. NLRP13 is a member of NLRs containing PYRIN domain as an effector domain. Its expression is conserved in primates and various mammals, but not in rodents. It is a novel protein and there is not a single dedicated article in the literature. Its information can only be achieved from a limited number of sources and the studies of our former lab members. Based on its expression in oocytes, it is suggested that NLRP13 is a maternal-effect gene. We have shown that NLRP13 is involved in inflammasome formation. After LPS/ATP treatment or *P. aeruginosa* infection, NLRP13 is upregulated in THP-1 monocytes, and proinflammatory cytokine secretion increases in stable THP-1 macrophages. NLRP13 is cleaved by Caspase-8 activated upon Fas/FasL-mediated FADD recruitment, and the cleaved C-terminal of NLRP13 is partly localized to mitochondria. NLRP13 do not directly involve in pyroptosis via Caspase-8, and PARP-1 cleavage, an apoptosis marker, is decreased in NLRP13-stable THP-1 cells after Caspase-8 is inhibited. In this thesis, the main aim of the study is to identify the novel interaction partners of NLRP13 so that to propose a notion about its role in signaling pathways and its molecular function. To achieve this goal, NLRP13-FLAG-stable THP-1 and Tera-2 cell lines were generated. Co-immunoprecipitation of NLRP13 from stable THP-1 monocytes, LPS/ATP-treated stable THP-1 macrophages and stable Tera-2 cells was performed with FLAG antibody followed by mass spectrometry. Due to various glitches, the results of repeated experiments could not be reached. However, the analysis of the obtained immunoprecipitates continues.

ÖZET

NLRP13 PROTEİNİN ETKİLEŞİM ORTAKLARININ ARAŞTIRILMASI

NOD-benzeri reseptörler (NLR'ler), örüntü tanıma reseptör ailesinin sitoplazmik üyeleridir ve geniş ölçüde iltihaplanma oluşumunda, sinyal iletiminde, transkripsiyon aktivasyonunda, hücre ölümünde, üremede ve embriyonik gelişimde işlev görür. NLRP-13, efektör bölgesi olarak PYRIN bölgesi içeren NLR'lerin bir üyesidir. İfadesi primatlarda ve çeşitli memelilerde korunurken kemirgenlerde korunmaz. Literatürde hakkında hiçbir makale bulunmayan yeni bir proteindir. Bilgilerine sadece sınırlı sayıda kaynaktan ve eski laboratuvar üyelerimizin çalışmalarından ulaşılabilir. Oositlerdeki ifadenmesine dayanarak, NLRP13'ün maternal etkili bir gen olduğu ileri sürülmektedir. Bizim bulgularımıza göre NLRP13'ün inflammatuar oluşumunda rol aldığı belirlenmiştir. LPS/ ATP tedavisinden veya *P. aeruginosa* enfeksiyonundan sonra, NLRP13 seviyesi THP-1 monositlerinde yukarı regüle edilir ve proinflammatuar sitokin salgılanması NLRP-13-stabil THP-1 makrofajlarında artar. NLRP13 ayrıca Fas/FasL aracılı FADD alımıyla aktive edilen Kaspaz-8 tarafından kesilir ve NLRP13'ün bölünmüş C-terminali kısmen mitokondride lokalize olur. NLRP13, Kaspaz-8 yoluyla olan piroptozda doğrudan yer almaz, ve kararlı THP-1 hücrelerinde Kaspaz-8 inhibe edildikten sonra apoptozun ayırt edici özelliği olan PARP-1 kesilimi azalır. Bu tezdeki çalışmanın temel amacı, sinyal yollarındaki rolü ve moleküler işlevi hakkında bir fikir önermek için NLRP13'ün yeni etkileşim ortaklarını belirlemektir. Bu amaca ulaşmak için, NLRP13-FLAG-stabil THP-1 ve Tera-2 hücre hatları üretildi. NLRP13'ün stabil THP-1 ve stabil Tera-2 hücrelerinden ve LPS/ATP-tedavili stabil THP-1 makrofajlarından FLAG antikoruna ile immüno-çöktürme işlemi uygulandı ve ardından kütle spektrometrisi yapıldı. Çeşitli aksaklıklardan dolayı tekrarlı deney sonuçlarına ulaşamadı, ancak elde edilen immünçöktürmelerinin analizi devam etmektedir.

TABLE OF CONTENTS

ACKNOWLEDGEMENTS	iii
ABSTRACT	v
ÖZET	vi
LIST OF FIGURES	x
LIST OF TABLES	xiii
LIST OF SYMBOLS	xv
LIST OF ACRONYMS/ABBREVIATIONS	xvi
1. INTRODUCTION	1
1.1. Innate Immune System	1
1.2. Pattern Recognition Receptors	1
1.3. NOD-like Receptors	2
1.4. NLRP13	4
2. HYPOTHESIS AND PURPOSE	7
3. MATERIALS	8
3.1. Cell Lines	8
3.2. Chemicals and Buffers	9
3.2.1. Agarose Gel Electrophoresis	9
3.2.2. Culture of Bacteria	9
3.2.3. Cell Culture	10
3.2.4. Coomassie Blue Staining and Western Blotting	12
3.2.5. Co-immunoprecipitation	15
3.3. Fine Chemicals	16
3.3.1. Plasmids	16
3.3.2. Primers	17
3.3.3. Enzymes	18
3.3.4. Antibodies	18
3.3.5. Kits	19
3.3.6. Equipments	19
4. METHODS	21

4.1. Maintenance of Cell Lines	21
4.1.1. HEK293FT Cell Line	21
4.1.2. THP-1 Cell Line	21
4.1.3. Tera-2 Cell Line	21
4.2. Molecular Cloning	22
4.2.1. Generation of pENTR1A-NLRP13-FLAG	22
4.2.1.1. Polymerase Chain Reaction	22
4.2.1.2. DpnI Restriction Enzyme Digestion	24
4.2.1.3. Transformation	25
4.2.1.4. Analytical Digestion	25
4.2.1.5. Preparation of PCR Integration Samples for Sanger Sequencing	26
4.2.2. Generation of pLEX307-NLRP13-FLAG	26
4.3. Development of Stable Cell Lines	27
4.3.1. Lentivirus Production via Calcium Phosphate Transfection in HEK293FT Cells	27
4.3.2. Lentivirus Harvesting and Lentiviral Transduction of THP-1 Cells	27
4.4. PMA Differentiation of THP-1 cells and Treatments of THP-1 cells and PMA-differentiated THP-1 Macrophages	28
4.5. Total Protein Lysate Preparation	29
4.6. Coomassie Staining and Western Blotting	30
4.7. Flow Cytometry	31
4.8. Determination of Protein Concentration	31
4.9. Co-immunoprecipitation	32
4.10. Protein Elution from Gel Matrix	33
5. RESULTS	34
5.1. Endogenous Protein Expression Levels of NLRP13 in Human Cell Lines	34
5.2. Generation of Stable Lines	35
5.2.1. Cloning of 3X FLAG tag into pENTR1A-NLRP13 vector	35
5.2.2. Transduction of THP-1 and Tera-2 cells and validation of NLRP13-FLAG expression levels	39

5.3. Investigation of Interaction Partners of NLRP13	44
5.3.1. Co-immunoprecipitation of NLRP13 via FLAG antibody	44
5.3.2. Bioinformatic Analysis of NLRP13 Interaction Partners Using Mass Spectrometry Data	54
6. CONCLUSION AND DISCUSSION	55
REFERENCES	60
APPENDIX A: PLASMID MAPS	65

LIST OF FIGURES

Figure 1.1.	Classification of NLR Gene Family.	3
Figure 5.1.	Endogenous NLRP13 protein expression levels in different human cell lines. NLRP13: 119 kDa, β -Actin: 42 kDa.	34
Figure 5.2.	Confirmation of PCR amplification of the primers before PCR integration of 3XFLAG tag.	35
Figure 5.3.	Analytical digestion of PCR integration colonies with EcoRV and SacI restriction digestion enzymes after DpnI digestion.	36
Figure 5.4.	Linearization of pENTR1A-NLRP13-FLAG plasmid with NheI restriction digestion enzyme.	37
Figure 5.5.	Analytical digestion of pLEX307-NLRP13-FLAG colonies with BamHI restriction enzyme.	38
Figure 5.6.	An electropherogram of Sanger sequencing of one of the pLEX307-NLRP13-FLAG plasmids obtained from the colonies along with a representation of the reference sequence of the region containing 3XFLAG tag.	38
Figure 5.7.	Validation of NLRP13 and 3XFLAG tag protein expressions of pLEX307-NLRP13-FLAG plasmids via Western blotting.	39
Figure 5.8.	Transfection efficiency of HEK293FT cells transfected with pLEX plasmids and the packing plasmids for lentivirus production.	40

Figure 5.9.	Transduction of THP-1 cells.	41
Figure 5.10.	Transduction of Tera-2 cells.	42
Figure 5.11.	Validation of protein expression in NLRP13-FLAG-stable THP-1 cells via Western blotting by using anti-NLRP13 rabbit pAb and anti-FLAG mouse mAb.	43
Figure 5.12.	Validation of protein expression in NLRP13-FLAG-stable Tera-2 cells via Western blotting by using anti-NLRP13 rabbit pAb and anti-FLAG mouse mAb.	44
Figure 5.13.	Co-immunoprecipitation of NLRP13 eluted with Laemmli buffer.	45
Figure 5.14.	Optimization of co-immunoprecipitation of NLRP13.	46
Figure 5.15.	Co-immunoprecipitation samples eluted with glycine buffer were visualized via Coomassie Blue staining.	47
Figure 5.16.	Co-immunoprecipitation samples eluted with glycine buffer were detected by anti-NLRP13 rabbit pAb and anti- β -Actin rabbit mAb via Western blotting.	48
Figure 5.17.	Co-immunoprecipitation samples eluted with urea buffer were visualized via Coomassie Blue staining.	49
Figure 5.18.	Co-immunoprecipitation samples eluted with urea buffer were detected by anti-NLRP13 rabbit pAb and anti- β -Actin rabbit mAb via Western Blotting.	49

Figure 5.19. Protein expression levels in NLRP13-FLAG-stable THP-1 cells with or without PMA differentiation upon LPS/ATP treatment in a time-dependent manner.	51
Figure 5.20. Co-immunoprecipitation of NLRP13 from THP-1-NLRP13-FLAG macrophages and Tera-2-NLRP13-FLAG cells by anti-FLAG antibody visualized via Coomassie Blue staining.	52
Figure 5.21. Co-immunoprecipitation of NLRP13 from THP-1-NLRP13-FLAG macrophages and Tera-2-NLRP13-FLAG cells by FLAG antibody analyzed via Western blotting.	53
Figure 5.22. Mass spectrometry analysis of NLRP13-FLAG immunoprecipitation using anti-FLAG antibody.	54
Figure A.1. Map of the pENTR1A-NLRP13 vector.	65
Figure A.2. Map of the pLEX307 ccdB vector.	66

LIST OF TABLES

Table 3.1.	Cell lines used in this study.	8
Table 3.2.	Chemicals used in agarose gel electrophoresis.	9
Table 3.3.	Chemicals used in bacterial culture.	9
Table 3.4.	Cell culture chemicals.	10
Table 3.5.	Transfection and transduction reagents.	11
Table 3.6.	Chemicals and solutions used in Coomassie Blue staining and West- ern blotting.	12
Table 3.7.	Chemicals and buffers used in co-immunoprecipitation.	15
Table 3.8.	Plasmids.	16
Table 3.9.	Primers used in PCR integration and Sanger sequencing.	17
Table 3.10.	Enzymes and buffers for molecular cloning.	18
Table 3.11.	Antibodies.	18
Table 3.12.	Kits.	19
Table 3.13.	Equipments.	19
Table 4.1.	First PCR components.	22

Table 4.2.	First PCR conditions.	23
Table 4.3.	Second PCR components.	24
Table 4.4.	Second PCR conditions.	24

LIST OF SYMBOLS

°C	Degree Celcius
g	Gram
g	Gravity
h	Hour
kDa	Kilodalton
L	Liter
M	Molar
mg	Miligram
ml	Mililiter
mM	Milimolar
mm	Milimeter
min	Minute
ng	Nanogram
rpm	Revolutions per Minute
sec	Second
V	Voltage
α	Alpha
β	Beta
κ	Kappa
μg	Microgram
μl	Microliter
μM	Micromolar

LIST OF ACRONYMS/ABBREVIATIONS

Ab	Antibody
AD	Acidic Transactivation Domain
ALR	Absent in melanoma 2 (AIM)-like receptor
APS	Ammonium Persulfate
ASC	Apoptosis Associated Speck-like Protein Containing CARD
ATP	Adenosine Triphosphate
BIR	Baculoviral Inhibitory Repeat-like Domain
BSA	Bovine Serum Albumin
CARD	Caspase Activation and Recruitment Domain
Caspase	Cysteine-Aspartic Protease
CLR	C-type Lectin Receptor
DAMP	Danger Associated Molecular Patterns
dH ₂ O	Distilled Water
ddH ₂ O	Double-distilled Water
DMEM	Dulbecco's Modified Eagle Medium
DMSO	Dimethyl Sulfoxide
DNA	Deoxyribonucleic Acid
EDTA	Ethylenediaminetetraacetic Acid
EGFP	Enhanced Green Florescent Protein
FADD	Fas-associated Protein with Death Domain
FBS	Fetal Bovine Serum
GFP	Green Fluorescence Protein
HBS	Hepes Buffer Saline
HEK293	Human Embryonic Kidney Cells
IL	Interleukin
IgG	Immunoglobulin G
IP	Immunoprecipitation
LB	Luria Broth

LPS	Liipopolysaccharide
LRR	Leucin-rich Repeats
MHC	Major Histocompatibility Complex
mRNA	Messenger RNA
NACHT	Present in NAIP, CIITA, HET-E, and TP1
NaCl	Sodium Chloride
NEAA	Non-essential Amino Acid
NLR	NOD-like Receptor
NOD	Nucleotide-binding Oligomerization Domain
PAMP	Pathogen Associated Molecular Domain
PBS	Phosphate Buffer Saline
PBS-T	Phosphate Buffer Saline and Tween-20
PCR	Polymerase Chain Reaction
PMA	Phorbol 12-Myristate 13-Acetate
PRR	Pattern Recognition Receptor
PVDF	Polyvinylidene Fluoride
PYD	Pyrin Domain
RIPA	Radioimmunoprecipitation Assay
RLR	RIG-I-like Receptor
RNA	Ribonucleic Acid
RT	Room Temperature
SDS	Sodium Dodecyl Sulfate
SDS-PAGE	SDS-Polyacrylamide Gel Electrophoresis
TBS	Tris Buffered Saline
TBS-T	Tris Buffered Saline and Tween-20
TEMED	N,N,N',N'-Tetramethyl Ethylenediamine
TLR	Toll Like Receptor
TNF	Tumor Necrosis Factor
WB	Western Blot
WT	Wild Type

1. INTRODUCTION

1.1. Innate Immune System

The immune system is a biological defense system consisting of a complex network of various cells, tissues, and organs. It protects the host against foreign invaders including pathogens (i.e., bacteria, viruses, fungi, and parasites), cancer cells, and toxins [1]. The defense mechanism is comprised of two main lines - the innate immune system and the adaptive immune system.

The innate immune system is the first line of defense against the antigens the body encounters. It responds non-specifically through physical and chemical barriers and cellular defense. Physical and chemical barriers can be exemplified as skin, low pH, the complement system, and phagocytes, while cellular defense includes monocytes, macrophages, natural killer cells, and dendritic cells that carry pathogen-recognition receptors (PRRs) [2, 3]. In cellular innate immune response, the immune cells recognizing pathogens recruit more cells of the innate immune system to the infection or inflammation sites by inflammatory response including cytokines and chemokines to boost the innate immunity. These cells provide an immediate response against a broad range of pathogens and rapidly prevent spreading pathogens throughout the body [1,3].

1.2. Pattern Recognition Receptors

The innate immune system responds via germline-encoded pattern recognition receptors (PRRs) which are the crucial sensor proteins to recognize the molecular patterns of microorganisms and host/tissue damage. PRRs have mainly two classes that are membrane-bound receptors and cytoplasmic receptors. These receptors recognize pathogen-associated molecular patterns (PAMPs) including patterns of bacterial LPS, microbial DNA and viral RNA, and danger-associated molecular patterns (DAMPs) released from damaged or stressed cells such as uric acid, heat-shock proteins, mtDNA, extracellular ATP, amyloid β , S100, histones and extracellular matrix proteins [4,5].

PRRs include Toll-like receptors (TLRs) and C-type lectin receptors (CLRs) as membrane-bound receptors, and, nucleotide-binding oligomerization domain (NOD)-like receptors (NLRs), retinoic acid inducible gene I (RIG-I)-like receptors (RLRs) and absent in melanoma 2 (AIM2)-like receptors (ALRs) as cytoplasmic receptors, and other cytosolic DNA receptors as intracellular sensors [6–9].

PRRs recognizing their ligands transmit the signal to the downstream signaling pathways and orchestrate inflammatory response by recruiting intermediate proteins and secreting cytokines, chemokines, hormones, and growth factors [10].

1.3. NOD-like Receptors

Nucleotide-binding oligomerization domain (NOD)-like receptors (NLRs) are the cytoplasmic members of pattern recognition receptors. The NLRs are evolutionarily conserved intracellular sensors functioning in inflammasome formation, signal transduction, transcription activation, cell death, and also reproduction and embryonic development [11]. In humans, 22 NLRs are known, and serious human diseases caused by the mutations and single nucleotide polymorphisms (SNPs) in genes expressing NLRs indicate that NLRs have essential life-sustaining roles in the body [11].

NLRs have three main domains in their structures; N-terminal effector domain, central NOD, or NACHT (NAIP, CIITA, HET-E, TP-2) domain and C-terminal ligand-sensing leucine-rich repeats (LRR) domain [12]. NLRs have four subclasses based on their effector domain: NLRA with the acidic transactivation (AD) domain, NLRB with the baculoviral inhibition of apoptosis repeat (BIR) domain, NLRC with the caspase activation and recruitment (CARD) domain, and NLRP with the pyrin domain (Figure 1.1) [8].

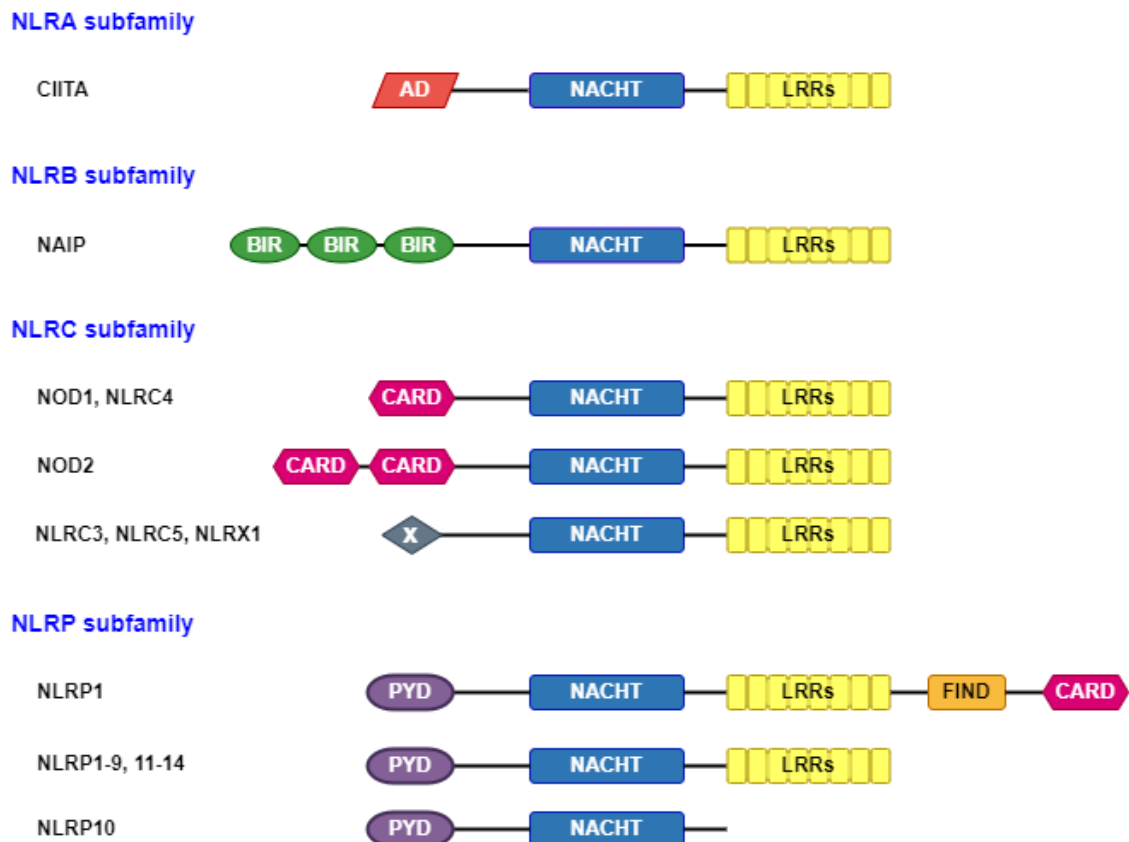


Figure 1.1. Classification of NLR Gene Family (Adapted from Kim *et al.*, 2016).

NLRA class consists of only one member, CIITA (MHC II transactivator) which regulates MHC-II expression. Its mutations are associated with lymphoid cancers [13]. NLRB class also has one member, NAIP (NLR family apoptosis inhibitor protein) which is known for its role in cell survival and bacterial defense and functions in flagellin sensing. NLRC class includes 6 members: NLRC1 (NOD1), NLRC2 (NOD2), NLRC3, NLRC4, NLRC5, and NLRX1. NOD1 and NOD2 function in RIP2-dependent NF- κ B and MAPK activation [12]. Their mutations are associated with several diseases such as asthma, dermal diseases, Crohn's disease, colon cancer, and tuberculosis [11, 12, 14]. NLRC3 is the negative regulator of TLR response and T cell activation while NLRC5 is the upregulator of MHC-I [12]. Besides the negative role of NLRC3 in TLR signaling, NLRC3 overexpression also leads to suppression of NF- κ B transcriptional activity and signaling via TRAF6 protein [15]. Its overexpression with NLRP3 inflammasome

components (NLRP3, ASC and Caspases 1 and 5) suppresses pro-Caspase-1 cleavage and IL-1 β processing suggesting that NLRC3 negatively regulates inflammatory responses [15].

Various types of NLRs are known to form inflammasome complex that is the multimeric complex activating immune response. In principle, the activation of the NLR recruits the apoptosis-associated speck-like protein containing CARD (ASC). They interact with their pyrin domain generating PYD-PYD interaction. The interaction recruits Caspase-1, and ASC and Caspase-1 are connected with CARD-CARD interaction. The inflammasome complex process the maturation of pro-inflammatory cytokines Il-1beta and Il-18 [16]. Among the NLRs, NLRP1-3, NLRP6, NLRP7, NLRP12, NAIP, and NLRC4 have been demonstrated to enable inflammasome formation [11,12].

The involvement of NLRs in reproduction and early-stage embryonic development is an emerging concept in recent studies. The phylogenetic analysis of the protein sequences of NLRs from various mammalian species along with mouse ortholog reveals NLRP2, 4, 5, 7-9, 11, 13 and 14 form a phylogenetic cluster separated from the other NLR clusters with immune roles [17]. To mention some of the studies on these proteins, the knockdown of NLRP2 mRNA in mouse oocytes leads to the arrest of early embryo development in early stages [18]. A mutation in NLRP2 is related to Beckwith-Wiedemann Syndrome which is a fetal overgrowth and human imprinting disorder [19]. In an *in vivo* study of NLRP5-null mice, NLRP5 is determined as a maternal-effect gene required for embryonic development beyond the two-cell stage [20]. NLRP7 is also a maternal-effect gene that has control on early development [21]. Its mutations cause hydatidiform mole, an inherited pregnancy failure in human [22]. NLRP14 is another NLR known in spermatogenesis and mutations in the gene cause spermatogenic failure in patients [23].

1.4. NLRP13

NLRP13, NOD-like receptor family pyrin domain containing 13, is an intracellular protein as a member of the NACHT/NOD, PYD, and LRR containing protein (NLRP)

family. NLRP13 gene, also known as NALP13, NOD14, PAN13 and CLR19.7, is conserved in chimpanzees, Rhesus monkeys, dogs, and cows, and absent in rodents. It is located on 19q13.43 in the human chromosome and has 12 exons. The molecular weight of the encoded protein from NLRP13 gene is 118.8 kDa. N-terminus of NLRP13 protein has a pyrin domain (PYD), followed by the central NACHT/NOD domain, and C-terminal leucine-rich repeat (LRR) domain.

NLRP13 is considered to be a maternal-effect gene that is highly expressed in oocytes, and its expression decreases progressively in embryos with a very low level in day5 embryos [24]. The mRNA expression of NLRP13 is enhanced by *Toxoplasma gondii* infection in THP-1 macrophages [25]. In another study, NLRP13 missense mutation is identified in doxorubicin-resistant U87 glioblastoma cell line, so that, NLRP13 is related to the regulation of NF- κ B activation [26]. In a study of immunological profiling of HIV-Tuberculosis co-infection, HIV- and TB-infected patients had significantly lower NLRP13 expression in deceased patients than in survivors [27].

The most detailed study of NLRP13 were obtained by our lab members. In the study of Gültekin, the localization experiments showed that NLRP13 is mainly in cytoplasm and conceivably in mitochondria [28]. In the co-immunoprecipitation experiments in overexpression conditions, it was shown that NLRP13 weakly interacts with inflammasome components, ASC and Caspase 1, but not with Caspase 5. Additionally, co-localization experiments showed that it forms inflammasome-like structures with ASC and Caspase-1 [28]. Yalçinkaya showed that NLRP13 protein expression is decreased when it is co-transfected with Caspase 8 or 9, the initiator caspases of extrinsic and intrinsic apoptotic pathways, respectively, in HEK293FT cells. Moreover, LPS and ATP are determined as the upstream regulators of NLRP13, and upon LPS/ATP treatment, NLRP13 leads to increase proIL-1 β and mature IL-1 β levels [29]. Yılmazer showed that NLRP13 generates a *Pseudomonas aeruginosa*-specific innate immune response, and upon both LPS/ATP treatment and *P. aeruginosa* infection, the secretion levels of pro-inflammatory cytokines of NLRP13-stable THP-1 macrophages are increased compared to noninfected PMA-differentiated cells. In *in vitro* cleavage assay, NLRP13 shows a correlation with Caspase-8 [30]. Recently, Çıracı demonstrated that

NLRP13 is cleaved by Caspase-8 which is activated upon FADD recruitment following Fas ligand binding to Fas receptor, and the cleaved C-terminal of NLRP13 is partly localized to mitochondria [31]. It was also shown that NLRP13 does not have an effect on macrophage polarization in THP-1 macrophages [31]. Çakır was studied the role of NLRP13 in cell death. It was shown that NLRP13 does not directly involve in pyroptosis via Caspase-8 [32]. However, PARP-1 cleavage, a hallmark of apoptosis, is decreased in NLRP13-stable THP-1 cells in which Caspase-8 is inhibited [32]. So, the results suggest NLRP13 could be involved in the molecular switch mechanism between apoptosis and pyroptosis via Caspase-8 activation complex [32].

2. HYPOTHESIS AND PURPOSE

NOD-like receptors (NLRs) are the cytoplasmic members of pattern recognition receptor family, broadly functioning in inflammasome formation, signal transduction, transcription activation, cell death, reproduction, and embryonic development. NLRP13 is a member of NLR family containing a PYRIN domain as an effector domain. It is highly expressed in oocytes, and its expression is decreased progressively in embryos. Based on its expression in oocytes, it is suggested that NLRP13 is a maternal-effect gene. It is also in the same cluster as reproduction-related NLRs phylogenetically. In our lab, it is determined that NLRP13 is involved in inflammasome formation and pro-inflammatory cytokine secretion and related to caspase cleavage. The C-terminal of NLRP13, which emerged after NLRP13 cleavage by Caspase-8 activated upon Fas/FasL-mediated FADD recruitment, is partly localized to mitochondria. NLRP13 do not directly involve in pyroptosis via Caspase-8, and PARP-1 cleavage, an apoptosis marker, is decreased in NLRP13-stable THP-1 cells after Caspase-8 is inhibited. Nonetheless, the role of NLRP13 in the cellular processes remains to be elucidated. The main aim of the thesis is to identify the novel interaction partners of NLRP13 and to propose a possible role in signaling pathways and its molecular functions. Tera-2 cell line, a human embryonal carcinoma cell line, and THP-1 cell line, a human leukemia monocytic cell line, were determined to express endogenous NLRP13. These cell lines were expected to give an idea about the potential interaction partners of NLRP13 in early embryonic development and innate immune response, respectively, and about the potential relevance to mitochondrial pathways. To achieve this goal, NLRP13-FLAG-stable THP-1 and Tera-2 cell lines were aimed to be generated. Co-immunoprecipitation of NLRP13 with FLAG antibody from NLRP13-FLAG-stable THP-1 and Tera-2 cells was also aimed to perform followed by mass spectrometry.

3. MATERIALS

3.1. Cell Lines

Table 3.1. Cell lines used in this study.

Cell Line	Main Source	Catalog Number	Provider
HEK293FT	Invitrogen, USA	R700-07	Kind gift of Prof. Maria Soengas, Spanish National Cancer Research Center, Spain
THP-1	ATTC, USA	ATCC TIB-202	Kind gift of Prof. Ahmet Gül, Istanbul University, Turkey
Tera-2	ATTC, USA	ATCC HTB-106	ATCC, USA

3.2. Chemicals and Buffers

3.2.1. Agarose Gel Electrophoresis

Table 3.2. Chemicals used in agarose gel electrophoresis.

Chemicals/Solutions	Supplier/Recipe
50X TAE	242 g Tris Base 57.1 ml Acetic acid 18.5 g EDTA up to 1 L ddH ₂ O
1% Agarose Gel	100 ml 1X TAE Buffer, 1 g Agarose
Agarose	Merck, Germany
Ethidium Bromide	Sigma-Aldrich, Germany
GeneRuler DNA Ladder Mix	Thermo Fischer Scientific, USA
Gel Loading Dye, Purple (6X)	NEB, USA

3.2.2. Culture of Bacteria

Table 3.3. Chemicals used in bacterial culture.

Chemicals	Supplier
LB Medium	Sigma-Aldrich, Germany
LB Agar	Sigma-Aldrich, Germany
Ampicillin (100 mg/ml)	AppliChem, Germany
Kanamycin (50 mg/ml)	AppliChem, Germany

3.2.3. Cell Culture

Table 3.4 Cell culture chemicals.

Reagents	Supplier/Recipe
Dulbecco's Modified Eagle Medium (DMEM), high glucose	Pan, PAN-Biotech, Germany
RPMI 1640	Gibco, Thermo Fischer Scientific, USA
RPMI 1640	Pan, PAN-Biotech, Germany
McCoy's 5A Medium with L-Gln	Pan, PAN-Biotech, Germany
FBS	Gibco, Thermo Fischer Scientific, USA
MEM NEAA – 100X	Gibco, Thermo Fischer Scientific, USA
Penicillin-Streptomycin (10,000 U/mL)	Gibco, Thermo Fischer Scientific, USA
DMSO	AppliChem, Germany
PMA	Sigma, USA
LPS	Sigma, USA
ATP	Sigma, USA
0.05% Trypsin	0.53 mM EDTA 0.5 g Trypsin 8 g NaCl 0.4 g KCl 0.06 g KH ₂ PO ₄ 0.048 g Na ₂ HPO ₄ 0.35 g NaHCO ₃ 1 g Glucose up to 1 L ddH ₂ O pH: 8.0, use filtered

Table 3.4 Cell culture chemicals (cont.).

Reagents	Supplier/Recipe
10X PBS	80 g NaCl 2 g KCl 14.4 g Na ₂ HPO ₄ 2.4 g KH ₂ PO ₄ up to 1 L ddH ₂ O pH: 7.2-7.4

Table 3.5. Transfection and transduction reagents.

Reagents	Supplier/Recipe
CaCl ₂	Merck, USA
Chloroquine diphosphate	AppliChem, Germany
HEPES	Gibco, Thermo Fischer Scientific, USA
PVDF 0,45 μ m	Roche, Germany
Polybrene	Sigma-Aldrich, Germany
Puromycin	Sigma-Aldrich, Germany
25 mM Chloroquine	0.129 g in 10 ml ddH ₂ O
2M CaCl ₂	11.098 g in 50 ml ddH ₂ O
2X HBS Buffer	50 mM HEPES 280 mM NaCl 1.5 mM Na ₂ HPO ₄ pH: 7.05

3.2.4. Coomassie Blue Staining and Western Blotting

Table 3.6. Chemicals and solutions used in Coomassie Blue staining and Western blotting.

Chemicals/Solutions	Supplier/Recipe
Acrylamide: Bisacrylamide	Applichem, Germany
Ammonium Persulfate	10% APS (w/v)
Tetramethylethylenediamine (TEMED)	Merck, Germany
Sodium Dodecyl Sulfate (SDS)	BioRad, USA
Sodium Dodecyl Sulphate (SDS) Solution 10% (w/v)	AppliChem, Germany
β -Mercaptoethanol	Merck, Germany
Bromophenol Blue	Merck, Germany
Sodium Chloride (NaCl)	Merck, Germany
Tris-HCl	Sigma-Aldrich, USA
Tris-Base	Sigma-Aldrich, USA
PageRuler Prestained Protein Ladder, 10 to 180 kDa (ref:26616)	Thermo Fisher Scientific, USA
Protease Inhibitor Cocktail	Roche, Germany
RIPA Lysis Buffer	50 mM Tris-HCl (pH:7.4) 150 mM NaCl 1% NP-40 (v/v) 0.5% Sodium deoxycholate (v/v) 0.1% SDS (v/v) Protease Inhibitor Cocktail

Table 3.6. Chemicals and solutions used in Coomassie Blue staining and Western blotting (cont.).

Chemicals/Solutions	Supplier/Recipe
5X Laemmli Sample Buffer	4 ml 1.5 M Tris-HCl, pH:6.8 5 ml 2-Mercaptoethanol 2 g SDS 10 ml Glycerol 1 ml 1% Bromophenol blue up to 20 ml ddH ₂ O
Coomassie Blue Staining Solution	0.1% Coomassie Brilliant Blue R-250 (w/v) 50% Methanol 10% Acetic acid in ddH ₂ O
Coomassie Blue Destaining Solution	50% Methanol 10% Acetic acid in ddH ₂ O
4% Stacking Gel	487 μ l 30% Acrylamide solution 750 μ l 1 M Tris-HCl, pH:6.8 30 μ l 10% SDS (w/v) 3 μ l TEMED 30 μ l 10% APS (w/v) 1.68 ml ddH ₂ O
12% Resolving Gel	3.2 ml Acrylamide solution 2 ml 1.5 M Tris-HCl, pH:8.8 80 μ l 10% SDS (w/v) 8 μ l TEMED 80 μ l 10% APS (w/v) 2.6 ml ddH ₂ O
2-Propanol	Merck, USA

Table 3.6. Chemicals and solutions used in Coomassie Blue staining and Western blotting (cont.).

Chemicals/Solutions	Supplier/Recipe
10X SDS Running Buffer	144.1 g Glycine 30.3 g Tris Base 10 g SDS (1% (w/v)) up to 1 L ddH ₂ O
PVDF Membrane	Merck Millipore, Germany
Methanol	Merck, USA
TWEEN-20	Sigma-Aldrich, USA
10X Wet Transfer Buffer	144.1 g Glycine 30.3 g Tris Base up to 1 L ddH ₂ O
1X Wet Transfer Buffer	10% (v/v) 10X Wet Transfer Buffer 20% (v/v) Methanol pH: ~9.0, cold use (-20°C)
10X TBS	24 g Tris Base 88 g NaCl in 1 L ddH ₂ O, pH: 7.6
1X TBS-T (0.1%)	1 L 1X TBS 1 ml Tween-20
Blocking solution	5% (w/v) non-fat milk in TBS-T
Bovine Serum Albumin Fraction V	Roche, Germany
5% (w/v) BSA	Bovine serum albumin fraction V in TBS-T

Table 3.6. Chemicals and solutions used in Coomassie Blue staining and Western blotting (cont.).

Chemicals/Solutions	Supplier/Recipe
Stripping Buffer (Mild)	1.5 g Glycine 0.1 g SDS 1 ml Tween-20 up to 100 ml ddH ₂ O, pH: 2.2
WesternBright ECL HRP substrate	Advansta, USA
WesternBright Sirius HRP substrate	Advansta, USA

3.2.5. Co-immunoprecipitation

Table 3.7 Chemicals and buffers used in co-immunoprecipitation.

Chemicals/Solutions	Supplier/Recipe
EDTA	Merck, Germany
Urea	Merck, Germany
Glycine	AppliChem, Germany
Potassium chloride (KCl)	Merck, Germany
Protein A/G Agarose beads	Thermo Fischer Scientific, USA
0.2% NP-40 lysis buffer	50 mM Tris-HCl, pH: 7.4 137 mM NaCl 0.2% NP-40 (v/v) 2 mM EDTA Protease inhibitor cocktail
Glycine Elution Buffer	0.1 M Glycine, pH: 2.5-3
Neutralization Buffer	1 M Tris, pH: 9.5

Table 3.7 Chemicals and buffers used in co-immunoprecipitation (cont.).

Chemicals/Solutions	Supplier/Recipe
Pre-urea Wash Buffer	50 mM Tris, pH: 8.5 1 mM EGTA 75 mM KCl
Urea Elution Buffer	7 M Urea 20 mM Tris, pH:7.5 100 mM NaCl
Urea Elution Buffer 2	8 M Urea 50 mM Tris-HCl 100 mM NaCl pH: 8

3.3. Fine Chemicals

3.3.1. Plasmids

Table 3.8. Plasmids.

Plasmid	Provider
pEGFP-C3	Retina Lab, Boğaziçi University
pcDNA3-FLAG-NLRP13	AKIL, Boğaziçi University
pENTR1A-NLRP13	AKIL, Boğaziçi University
pLEX307 cdb	Addgene, USA
pLEX307-GFP	AKIL, Boğaziçi University

3.3.2. Primers

Table 3.9. Primers used in PCR integration and Sanger sequencing.

Primer	Sequence (5' to 3')	Application
C-3XFLAG _pLEX307 _NLRP13_F	TGAAAAAGTCGACATGCAGGCTG CAGAAACTCGGGGACTACAAGGA CGACGATGACAAGGGATCCGACT ACAAGGACGACGATGACAAG	PCR Integration
C-3XFLAG _pLEX307 _NLRP13_R	TTTGTACAAGAAAGCTGGGTCTA GATATCTCATTACTTGTCATCGT CGTCCTTGTAGTCCTTGTCATCG TCGTCCTTGTAGTCGGATCC	PCR Integration
pENTR-F	CTACAAACTCTTCCTGTTAGTTAG	Sequencing
pENTR-R	ATGGCTCATAACACCCCTTG	Sequencing
NLRP13_Seq_F1	AGAAGCAGCAGCAGGGAATA	Sequencing
NLRP13_Seq_F2	GGTTCCCCTGGCTACCTTAC	Sequencing
NLRP13_Seq_F3	CATTCCACAAAGCCACAAGA	Sequencing
NLRP13_Seq_F4	ACGTGCAAATCGGTA ACTCC	Sequencing
NLRP13_Rev_Seq	AGTAGGCGCTGCAGTTCCTC	Sequencing

3.3.3. Enzymes

Table 3.10. Enzymes and buffers for molecular cloning.

Enzymes/Buffers	Supplier
Restriction Enzymes (DpnI, NheI, EcoRV-HF, SacI, BamHI-HF)	NEB, USA
Q5 High Fidelity Polymerase	NEB, USA
Q5 Polymerase Buffer 5X	NEB, USA
Gateway LR Clonase II Plus, Enzyme Mix	Invitrogen, USA

3.3.4. Antibodies

Table 3.11. Antibodies.

Antibody	Host	Supplier	Catalog Number	Application
Anti-Mouse IgG, HRP	Horse	Cell Signaling Technology, USA	7076S	WB, Co-IP
Anti-Rabbit IgG, HRP	Goat	Cell Signaling Technology, USA	7074S	WB
β -Actin	Rabbit mAb	Cell Signaling Technology, USA	4970S	WB
NLRP13	Rabbit	Abcam, UK	ab105410	WB
FLAG, M2	Mouse mAb	Sigma-Aldrich, Germany	F3165	WB, Co-IP

3.3.5. Kits

Table 3.12. Kits.

Kits	Supplier
NucleoSpin® Gel and PCR Clean-up Kit	Macherey Nagel, Germany
NucleoSpin® Plasmid Kit	Macherey Nagel, Germany
Pierce™ BCA Protein Assay Kit	Thermo Fisher Scientific, USA

3.3.6. Equipments

Table 3.13 Equipments.

Autoclaves	MAC601, Eyela, Japan ASB260T, Astekk, UK
Centrifuges	Allegra X22-R, Beckman, USA Himac CT4200C, Hitachi Koki, Japan J2-MC Centrifuge, Beckman, USA J2-21 Centrifuge, Beckman, USA
Freezers	2021D, Uğur, Turkey 4250T Uğur, Turkey
Flow Cytometer	BD Accuri C6, USA
Incubator	PHC Europe B.V, The Netherlands
Heat Block	Thermal Shake lite, VWR, USA
Micropipettes	Rainin Mettler Toledo, USA Axygen, USA, Axypipettes, USA
Microscopes	Nikon, Eclipse TS100, Netherlands
Microwave Oven	Arçelik, Turkey
Oven	Gallenkamp 300, UK
pH Meter	Hanna Instruments, USA
Pipettors	VWR, USA

Table 3.13 Equipments (cont.).

SDS-PAGE Electrophoresis System	Mini-Protean 4Cell BIO-RAD, USA
Power supply	Power Pac Universal, BIO-RAD, USA
SDS-PAGE Transfer Systems	Mini Trans-Blot Cell Trans-blot Semi-Dry BIO-RAD, USA
Shaker	Polymax USA Heildophl, Germany
Softwares	ImageJ, NIH, USA FlowJo, USA Syngene-Genetools, UK
Spectrophotometer	Nanodrop ND-100 Thermo, USA
Tube Rotator	Globe Scientific, USA
Thermal Cyclers	BIO-RAD, USA
Vortex	GmcLab, Gilson, USA
Water Bath	GFL, Germany
Water filter	UTES, Turkey
Western Blot and Agarose Gel Visualization	Syngene GBOX, UK

4. METHODS

4.1. Maintenance of Cell Lines

4.1.1. HEK293FT Cell Line

HEK293FT cell line is an adherent cell line derived from human embryonic kidney cells. HEK293FT cells were cultured in DMEM supplemented with 10% FBS, 1% MEM NEAA, and 0.5% Penicillin-Streptomycin (10,000 U/ml) in an incubator at 37°C supplying 5% CO₂ in air atmosphere. The cells were frozen in complete DMEM medium with 10% DMSO and 20% FBS and stored at -80°C.

4.1.2. THP-1 Cell Line

THP-1 cell line is a human monocytic cell line derived from a patient with acute monocytic leukemia. THP-1 cells are suspension cells and were cultured in RPMI 1640 supplemented with 10% FBS, 1% MEM NEAA, and 0.5% Penicillin-Streptomycin (10,000 U/mL) in an incubator at 37°C supplying 5% CO₂ in air atmosphere. The cells were frozen in complete DMEM medium with 10% DMSO and 20% FBS and stored at -80°C, or frozen in FBS with 10% DMSO and held at -150°C.

4.1.3. Tera-2 Cell Line

Tera-2 cell line is a human teratocarcinoma cell line. Tera-2 cells have an adherent phenotype and were maintained in McCoy's 5A supplemented with 15% FBS, 1% MEM NEAA, and 0.5% Penicillin-Streptomycin (10,000 U/ml) in an incubator at 37°C supplying 5% CO₂ in air atmosphere. The cells were frozen in complete DMEM medium with 10% DMSO and 20% FBS and stored at -80°C, or frozen in FBS with 10% DMSO and held at -150°C. All the cell lines were periodically checked for the absence of mycoplasma contamination.

4.2. Molecular Cloning

4.2.1. Generation of pENTR1A-NLRP13-FLAG

4.2.1.1. Polymerase Chain Reaction. PCR integration experiment was performed to clone 3X-FLAG tag containing BamHI restriction site into the C terminal of pENTR1A-NLRP13 plasmid. Two sequential PCR were performed for integration. The first PCR was to generate megaprimers that are the primer-dimers in the full length of the sequence to integrate and was to use as the primers for the second PCR. The primers designed including a homology arm to the integration site in pENTR1A-NLRP13 plasmid were purchased from Macrogen. The reaction was carried out in 50 μ l of reaction mixture containing 0.5 μ l of 100 μ M forward primer, 0.5 μ l of 100 μ M reverse primer, 0.5 μ l of 10 μ M dNTP, 10 μ l of 5X Q5 Buffer and 0.5 μ l of Q5 enzyme shown in Table 4.1 and the reaction conditions were shown in Table 4.2.

Table 4.1. First PCR components.

Components	Volume (μl)
3XFLAG Forward Primer (100 μM)	0.5
3XFLAG Reverse Primer (100 μM)	0.5
dNTP (10 mM)	0.5
Q5 buffer (5X)	10
Q5 Polymerase	0.5
ddH₂O	Up to 50
Total	50

Table 4.2. First PCR conditions.

Temperature (°C)	Duration	Cycle
98	3 min	1
95	30 sec	30
60	30 sec	
72	10 sec	
72	3 min	1
4	∞	

The PCR product was loaded into 0.7% agarose gel and run at 120 V for 40 minutes. The gel was visualized under UV light, and once the bands were confirmed, the desired bands were cut out on a UV box and weighed. The PCR product was extracted via NucleoSpin Gel and PCR Clean-up Kit (Macherey Nagel) and the concentration was measured by NanoDrop. For long-term storage, the extracted megaprimers were stored at -20°C.

The second PCR was performed to integrate 3X-FLAG tag into the C terminal of pENTR1A-NLRP13 plasmid. The reaction was carried out in 50 μ l of reaction mixture containing 250 ng of first PCR product, 50 ng of template plasmid, 1.5 μ l of 10 μ M dNTP, 5 μ l of 5X GC enhancer, 10 μ l of 5X Q5 Buffer, and 1 μ l of Q5 enzyme shown in Table 4.3 and the reaction conditions were shown in Table 4.4.

Table 4.3. Second PCR components.

Components	Volume (μl)/Amount
First PCR product (100 μM)	250 ng
Template plasmid (100 μM)	50 ng
dNTP (10 mM)	1.5
GC enhancer	5
Q5 buffer (5X)	10
Q5 Polymerase	1
ddH₂O	Up to 50
Total	50

Table 4.4. Second PCR conditions.

Temperature ($^{\circ}$C)	Duration	Cycle
98	3 min	1
95	60 sec	25
60	30 sec	
72	3 min	
72	3 min	1
4	∞	

The PCR product was cleaned up via NucleoSpin® Gel and PCR Clean-up Kit (Macherey Nagel). 20 μ l of ddH₂O was used in the elution step and the concentration was measured by NanoDrop. For long-term storage, the plasmid DNA was stored at -20°C.

4.2.1.2. DpnI Restriction Enzyme Digestion. For the plasmid DNA obtained from the second PCR, DpnI (NEB, USA) digestion reaction was performed. 50 μ l of DpnI reaction was prepared to contain 14 μ l of template DNA, 1 μ l of DpnI restriction enzyme, 5 μ l of CutSmart buffer(10X), and up to 50 μ l of ddH₂O. The same reaction

was also prepared for negative control using 50 ng of the pENTR1A-NLRP13 plasmid. Another negative control reaction was performed for both reactions without using the DpnI restriction enzyme. They were incubated at 37°C for 5 hours, and then, heat inactivation was applied at 80°C for 20 minutes.

4.2.1.3. Transformation. Top10 strain of *Escherichia coli* competent cells was thawed on ice. 10 μ l of DpnI digestion reaction was mixed with the cells by gentle pipetting. The mixture was incubated on ice for 15 minutes. Heat shock was performed in a water bath at 42°C for 60 seconds and immediately taken into ice, then, kept for 2 minutes. 950 μ l of Luria Broth (without antibiotic) was added to the bacteria cells and incubated at 37°C for 45-60 minutes by shaking. Afterward, the cells were centrifuged at 4500 rpm for 5 minutes. The supernatant was discarded leaving 100 μ l in the eppendorf. The pellet was resuspended and spread onto a 10-cm LB agar plate at RT containing kanamycin which is the selection antibiotic for pENTR1A plasmid. The plates were incubated at 37°C for 12-16 hours. On the next day, the plates were kept at 4°C until used to avoid satellite colony growth.

4.2.1.4. Analytical Digestion. Single colonies were selected and inoculated into 10 ml LB culture with kanamycin in 50-ml falcon. The cultures in the falcon, slightly loosening the cap, were incubated at 37°C for 12-16 hours by shaking. The next day, before plasmid isolation, glycerol stock was prepared with 800 μ l of the bacterial culture by adding 200 μ l of 70% glycerol. Plasmid isolation was performed using NucleoSpin® Plasmid Kit (Macherey Nagel) through the manufacturer's instructions. Analytical digestion reactions at the 25 μ l of final volume were performed for isolated plasmid DNA using EcoRV and SacI enzymes (NEB, USA) considering NEB's instructions. Uncut and single-cut reactions were also prepared as controls. The products were loaded into 1% agarose gel. The gel was run at 120 V for 40 minutes, and then, visualized under UV light.

4.2.1.5. Preparation of PCR Integration Samples for Sanger Sequencing. 10 μl of the isolated plasmid DNA samples at the final concentration of 100 ng/ μl were sent to Macrogen for sequencing.

4.2.2. Generation of pLEX307-NLRP13-FLAG

After the confirmation of the pENTR1A-NLRP13-FLAG plasmid via sequencing, NLRP13-FLAG sequence was cloned to pLEX307 ccdB lentiviral expression vector by gateway cloning. To this end, Gateway™ LR Clonase™ II Plus Enzyme Mix (Invitrogen, USA) was used. 10 fmoles of pENTR1A-NLRP13-FLAG vector were used as the entry clone in the volume of 1 μl . Before using the pENTR1A-NLRP13-FLAG vector, this vector was linearized by using NheI restriction enzyme, and the linearization was confirmed by agarose gel electrophoresis. 20 fmoles of pLEX307 ccdB plasmid were used as the destination vector in the volume of 1 μl . These vectors were mixed in a PCR tube at RT and 8 μl of 1X TAE buffer, pH: 8.0 was added into the tube. LR Clonase™ II Plus Enzyme Mix was thawed on ice for 2 minutes and briefly vortexed. 2 μl of the enzyme mix was added to the vector mix, and the LR reaction was briefly vortexed twice and micro-centrifuged. A second reaction was prepared without LR Clonase™ II Plus Enzyme Mix as a negative control. The reactions were incubated for 16 hours at 25°C. To terminate the reaction, 1 μl of the Proteinase K Solution was added to the samples, briefly vortexed, and incubated for 10 minutes at 37°C.

After Gateway™ cloning, the samples were transformed to the Stbl3 strain of Escherichia coli competent cells as in the process mentioned above. For colony formation, ampicillin-containing LB agar plates were used for the selection of the colony expressing pLEX307-NLRP13-FLAG plasmid. 10 μl of the plasmid DNA samples isolated from the positive colonies at the final concentration of 100 ng/ μl were sent to Macrogen for sequencing. Analytical digestion was also performed as mentioned above using BamHI, HF enzyme (NEB, USA). The products were loaded into 1% agarose gel. The gel was run at 100 V for 50 minutes and visualized.

4.3. Development of Stable Cell Lines

4.3.1. Lentivirus Production via Calcium Phosphate Transfection in HEK293FT Cells

To produce lentiviruses, the expression plasmid and packaging vectors were transferred into HEK293FT cells via the calcium phosphate transient transfection method. For transfection, 3×10^6 cells HEK293FT cells were seeded into a 100 mm culture dish with 10 ml complete DMEM medium and incubated at 37°C, 5% CO₂ for 1-2 days until they reach 80-90% confluency. On the day of transfection, before preparing the transfection mixture, chloroquine with the final concentration of 25 μ M was added to the medium. The transfection mixture was prepared in an eppendorf in a total of 1 ml. Firstly, the proper volume of plasmids (2500 ng expression plasmid, 2250 ng pCMV delta R8.2 packaging plasmid, and 225 ng pCMV-VSV-g envelope plasmid) was mixed in ddH₂O. Then, 61 μ l of ice-cold 2M CaCl₂ was added drop by drop into the plasmid mixture. 500 μ l of 2X HBS buffer was subsequently added into the mixture and mixed immediately until the bubbles are formed. The mixture was incubated at room temperature for 10 minutes and added to the medium of cells drop by drop. After 6-8 hours, the medium with Cq is changed to complete medium. After 48 hours, the efficiency of transfection was examined under the fluorescence microscope.

4.3.2. Lentivirus Harvesting and Lentiviral Transduction of THP-1 Cells

At 48 hours post-transfection, lentivirus-containing media of the HEK293FT cells was harvested. The media was filtered with a 0.45 μ m filter tip, using a 10-ml syringe, and collected in a 15-ml falcon. The filtered virus-containing media was aliquoted to cryotubes as 1-ml aliquots and directly used for infection or stored at -80°C. All the cells and the materials used for virus production and transduction were bleached before discarding.

For transduction, 1×10^6 of THP-1 cells in 1 ml of the full RPMI medium were seeded to each well of a 6-well cell culture plate for each construct and the controls. In

the same day of seeding, 1 ml of the filtered virus-containing medium and polybrene to a final concentration of 4 $\mu\text{g}/\text{ml}$, after 5-minute incubation at RT, was added drop by drop to each well. The plate was centrifuged at 2900 rpm for 90 minutes.

For the transduction of Tera-2 cells, 6×10^5 of Tera-2 cells in 2 ml of full McCoy's 5A medium containing 15% FBS were seeded to each well of a 6-well cell culture plate 3 days before transduction. When the cells were reached 80-85% confluency, the medium was discarded and 1 ml of the filtered virus-containing medium with polybrene at a final concentration of 4 $\mu\text{g}/\text{ml}$ incubated for 5 minutes at RT was added drop by drop to each well. Total volume was completed to 2 ml with the full McCoy's 5A medium containing 15% FBS for each well.

After 24 hours, the virus-containing medium was changed with fresh medium for each cell line. On the third or fifth day of infection, puromycin (1 $\mu\text{g}/\text{ml}$) was started using for selection of the THP-1 and Tera-2 transduced cells, respectively, and continued until all the nontransduced cells were dead.

4.4. PMA Differentiation of THP-1 cells and Treatments of THP-1 cells and PMA-differentiated THP-1 Macrophages

For PMA differentiation, 2.5×10^6 THP-1 cells for each well of 6-well plate or 5×10^6 THP-1 cells for 100 mm cell culture plate were seeded with 20 ng/ml PMA in 2 or 10 ml of full RPMI medium containing 3% FBS, respectively. The PMA-containing medium was discarded after 24 hours of treatment, and the cells were washed with 1X PBS. Fresh full RPMI medium containing 10% FBS was added to the cells. The cells were allowed to differentiate for 48 hours. Approximately, 1 or 2 million(s) cells were supposed to collect from a well of 6-well plate or 100 mm cell culture plate after PMA differentiation, respectively. Before LPS/ATP treatment, 1×10^6 of THP-1 cells in 2 ml of full RPMI medium containing 10% FBS were also seeded in a well of 6-well plate. To activate the inflammasome formation, THP-1 cells and PMA-differentiated THP-1 macrophages were treated with 100 ng/ml LPS for 1-6 hours, and then, 2 mM ATP for 30 minutes.

4.5. Total Protein Lysate Preparation

For Western blotting, the cells were counted and 1×10^6 cells were centrifuged at 1000 rpm for 5 minutes for THP-1 cells and 1500 rpm for 3 minutes for Tera-2 cells. The supernatant was discarded, and the pellet was kept on ice. It was dissolved in 300 μ l of RIPA lysis buffer (50 mM Tris-HCl (pH:7,4), 150 mM NaCl, 1% NP-40 (v/v), 0.5% sodium deoxycholate (v/v), 0.1% of 10% SDS (v/v)) after adding 25X EDTA-free protease inhibitor cocktail (PIC, Roche). The cells were lysed for at least 20 minutes at -20°C . Then, 2X Laemmli buffer was added and boiled at 95°C for 10 minutes.

For HEK293FT cells, all the media was removed from the cell culture plate and the cells were washed gently with ice-cold PBS twice. Then, the PBS was aspirated and 200 μ l of PIC-containing RIPA lysis buffer was directly added to each cell culture well. The cells were incubated for at least 1 hour at -20°C . They were gathered using a cell scraper to scrape from the bottom of the dish or a tip with the help of their mucous form. The cell lysate was pipetted about 20 times to form a homogeneous lysate. The lysate was transferred to a 1.5-ml microcentrifuge tube and allowed to stand for 5 minutes on ice. The sample was centrifuged at 13000 rpm for 15 minutes at 4°C . The supernatant was transferred to a new tube. It was directly stored at -20°C for further experiments, or before storage, added 5X Laemmli buffer, and boiled at 95°C for 10 minutes.

For immunoprecipitation, an appropriate number of the cells were counted and centrifuged. The supernatant was discarded, and the pellet was kept on ice. The pellet was dissolved in up to 1 ml of 0.2% NP-40 lysis buffer (50 mM Tris-HCl (pH:7,4), 137 mM NaCl, 0.2% NP-40 (v/v), 2mM EDTA) after adding 25X EDTA-free protease inhibitor cocktail (PIC, Roche). The cells were lysed for at least 1 hour at -20°C . The cells lysed were centrifuged at 13000 rpm for 30 minutes at 4°C . The supernatant was used for the further process.

4.6. Coomassie Staining and Western Blotting

After the lysate preparation, total protein was run on SDS-PAGE gel. SDS-PAGE gel was prepared by pouring 12% resolving gel and 4% stacking gel solution, respectively, between two glasses providing the gel with 1.5-mm thickness. Isopropanol was used to overlay the surface of the resolving gel and discarded before pouring stacking gel solution. A proper comb was inserted to stacking gel solution ensuring not to form air bubbles near the wells. Polymerization was allowed for each gel for 20-30 minutes at RT. The gel was placed into a vertical tank, and the tank was filled with 1X running buffer. The samples were loaded into wells and run at 80V and 120V for the stacking and resolving steps, respectively.

For Coomassie staining, the gel was placed in a plastic tray containing Coomassie Blue staining solution and stained on an orbital shaker for 30 minutes-1 hour. After the staining, the gel was destained with Coomassie Blue destaining solution till blue protein bands were visible on a clear background. The destained gel was visualized using Gel Doc XR System (Bio-Doc, Italy).

For Western blotting, the wet transfer method was used to transfer the proteins to PVDF membrane with 0.2 nm pore size (Merck Millipore, Germany). Firstly, a sufficient amount of 1X wet transfer buffer was prepared to fill the transfer tank and equilibrate the filter papers, PVDF membrane and the gel and cooled. Filter papers and the gel were soaked in the transfer buffer. PVDF membrane was activated in methanol for 5 minutes, and then, placed into ddH₂O until being drenched. A transfer stack in a sandwich form was prepared with a cassette holder, two fiber foam pads (sponges), two filter papers, activated PVDF membrane and the gel. The gel side of the holder was placed facing the cathode (-) and the membrane side facing the anode (+). The stack was placed in the tank with ice block inside and the tank was filled with 1X wet transfer buffer. The transfer was performed at 100V for 2.5-3 hours. Subsequently, the membrane was placed in blocking solution (5% non-fat milk powder in TBS-T) on an orbital shaker and incubated for 1 hour at RT. Then, the membrane was placed in a 50-ml falcon containing a proper primary antibody diluted in 1:1000-1:2000 ratio

with 5% BSA in TBS-T and incubated on a rotator at 4°C for 12-16 hours. Lastly, the membrane was incubated in a proper HRP-linked secondary antibody diluted in 1:5000 ratio with blocking solution on a rotator for 1 hour at RT. Between all the incubation steps and after the secondary antibody incubation, the membrane was washed 3 times with 1X TBS-T for 5 minutes each.

For the visualization of the blotting, WesternBright ECL HRP or Sirius HRP substrate (Advansta) was used. Luminol/enhancer and chemiluminescent peroxide solutions were mixed in 1:1 ratio, and the membrane was agitated shortly in the mixture until the whole surface of the membrane was covered. The image of the membrane was captured using the SynGene-Genetools. Image analysis of the blotting results was performed by Fiji ImageJ software.

4.7. Flow Cytometry

2×10^5 cells of each sample were counted and centrifuged. The supernatants were aspirated, and the pellets were washed once with 1X PBS. Then, the pellet was dissolved in 300 μ l of 1X PBS and kept on ice. The cells were counted on BD Accuri C6 Flow Cytometer. Gating strategy was firstly on wild-type cells, and then to GFP+ cells. The data was analyzed using FlowJo v10.1 (BD Biosciences) software.

4.8. Determination of Protein Concentration

For the determination of protein concentration, BCA Protein Assay kit was performed, and for the protocol, the manufacturer's instructions (Pierce™ BCA Protein Assay Kit) were followed. Firstly, the BCA standards in different dilutions were prepared. For the long-term storage, the standards were kept at -20°C. Next, the samples were prepared in 1:1, 1:10 and 1:100 dilutions. 25 μ l of each standard and sample was added into the wells of 96-well cell culture plate. All the standards and the samples were duplicated. After adding, the working reagent (WR) was prepared in dark as mixing the reagent A and reagent B in 50:1 ratio. 200 μ l of WR was added into the standards and samples. The 96-well plate was covered with a piece of aluminum coil

and incubated at 37°C for 30 minutes. Before the absorbance measurement, the plate was cooled at RT for 5 minutes. The absorbance was measured on the plate reader at 562 nm.

4.9. Co-immunoprecipitation

For the immunoprecipitation experiments, all the protocol and the usage of the materials was performed on ice. Pierce™ Protein A/G Agarose beads were used for the precipitation. The bottle of Protein A/G Agarose was gently swirled to get a homogeneous suspension. 50 or 75 μ l of the resin was added into a microcentrifuge tube. The resin was washed for 5 times with 400 μ l of NP-40 lysis buffer. The tube was gently centrifuged on mini on-bench centrifuge at RT for 1 minute at each step to collect the beads. 5 or 7.5 μ l of anti-FLAG, M2 antibody diluted in 300 μ l of the lysis buffer was added to the beads and incubated on an eppendorf shaker for 2 hours by gently mixing. After 2 hours, the bead-antibody complex was washed with 400 μ l of the lysis buffer for 3 times. As total protein lysate, 15-40x10⁶ of NLRP13-FLAG-stable THP-1 cells or 2.5-5x10⁶ of NLRP13-FLAG-stable THP-1 macrophages or Tera-2 cells were collected and prepared following the total protein preparation protocol as mentioned above. After taking a sample as a whole cell lysate (WCL), the supernatant was added to the bead/antibody complex and incubated on an eppendorf rotator at 4°C overnight. Next day, the resin was centrifuged, and the supernatant was saved as flow-through (FT) sample. The lysate-bead/antibody conjugate was washed with the lysis buffer for 3 times. At all the steps, the wash buffer was removed carefully not to lose the beads or the complexes. Lastly, the beads were directly eluted using 50 μ l of the lysis buffer and 50 μ l of 2X Laemmli buffer. It was boiled at 95°C for 10 minutes.

As another method for elution, glycine buffer was performed. Subsequent to the last washing of the lysate-bead/antibody conjugate, 50 μ l of 0.1 M glycine, pH 2.5-3, was added to the beads and incubated for 10 minutes with frequent agitation. The beads were gently centrifuged and the elute was transferred into a new tube. The elute was neutralized with 5 μ l of 1 M Tris, pH 9.5.

For mass spectrometry analysis, urea elution was performed. For the first trial of mass spectrometry, after the last wash of the lysate-bead/antibody conjugate, the beads were washed with pre-urea wash buffer and centrifuged. All the supernatant was removed, and 5 volumes of 7M urea elution buffer were added to the tube. It was rotated on a rotator lobster for 30 minutes at RT. This step was repeated once more to ensure releasing most of the captured proteins. The beads were pelleted, and the supernatant was collected in a new tube. For the analysis, 5X Laemmli buffer was added to the beads in 50 μ l of the urea elution and boiled at 95°C for 10 minutes. Coomassie Blue staining and Western blotting were used for the analysis. After the confirmation of the pull-down, the samples were sent mass spectrometry. For the last trial of mass spectrometry, the lysate-bead/antibody conjugate was eluted via Laemmli elution and 80% of samples were run on SDS-PAGE gel. The proteins were eluted from gel following the protein elution from gel matrix protocol as mentioned below and sent mass spectrometry for analysis.

4.10. Protein Elution from Gel Matrix

The whole gel strip for each sample of interest was excised to elute proteins from the SDS-gel matrix. Each excised gel piece was placed in a clean mortar. 3 ml of elution buffer (50 mM Tris-HCl, 100 mM NaCl, 8 M Urea, pH:8) was added to completely immerse the gel piece. The gel pieces were crushed using a clean pestle and aliquoted into 1.5 or 2-ml microcentrifuge tubes. They were incubated on a rotary shaker at 30°C overnight. The next day, the samples were centrifuged at 10000 g for 15 minutes and the supernatant was carefully pipetted into a new centrifuge tube.

5. RESULTS

5.1. Endogenous Protein Expression Levels of NLRP13 in Human Cell Lines

NLRP13 is one of many NLR proteins whose molecular function is still unknown. To identify this, the initial aim is the determination of the endogenous protein expression levels in different cell lines, and of which NLRP13-expressing cells can be used in knockdown/knockout or overexpression experiments. By using the commonly used cell lines, NLRP13 expression levels was analyzed by Western blotting (Figure 5.1). For the analysis, THP-1, human leukemia monocytic cell line and Jurkat, immortalized T lymphocyte cell line, were used as immune cells. Jar, placental carcinoma cell line, Swan71, throphoblast cell line, Tera-2, human embryonal carcinoma, and Hec1a, endometrial carcinoma cell line, were as the cells of immune privilege sites and embryonic cells. B16, murine melanoma cell line, and HEK293FT, human embryonic kidney cell line, were used as negative control , and THP-1-NLRP13, NLRP13-overexpressing cell line, was used as positive control.

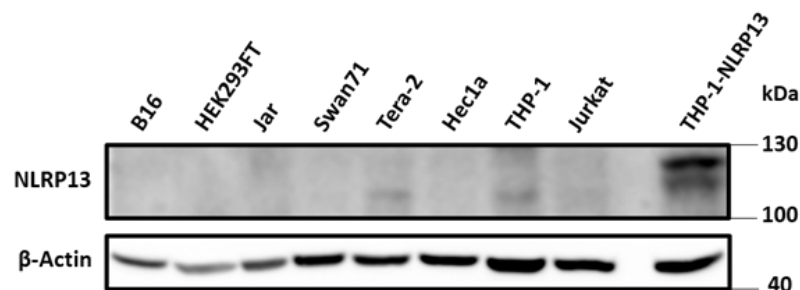


Figure 5.1. Endogenous NLRP13 protein expression levels in different human cell lines. NLRP13: 119 kDa, β -Actin: 42 kDa.

The calculated molecular weight of NLRP13 is 118.9. The band of NLRP13 was detected in THP-1 and Tera-2 cell lines. The positive control group, THP-1-NLRP13 cell line, had two bands slightly above the calculated NLRP13 band, probably

because of the transduction of the full length of NLRP13 and/or a post-translational modification.

5.2. Generation of Stable Lines

5.2.1. Cloning of 3X FLAG tag into pENTR1A-NLRP13 vector

For the immunoprecipitation experiments, the first aim was to add a 3X FLAG tag to the C-terminus of NLRP13. For this purpose, PCR integration method was used in the initial step. Forward and reverse primers were designed in a way of containing homology arms overlapping with NLRP13 sequence, a BamHI restriction digestion site for analytical digestion, and regions to overlap with each other. A PCR was carried out with these primers using them as a template. The expected band was 148 bp including 78 bp of 3X FLAG tag. The PCR product was confirmed on a 0.7% agarose gel (Figure 5.2).

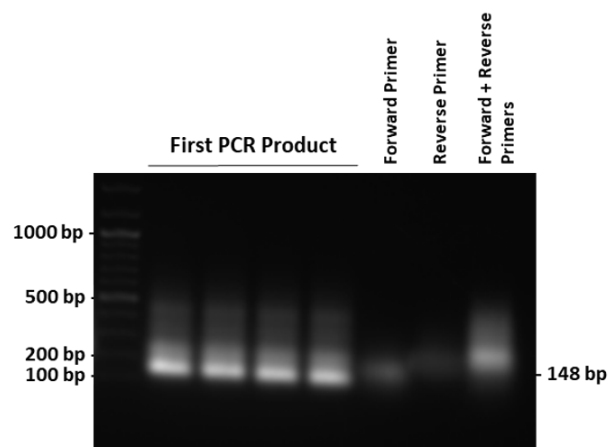


Figure 5.2. Confirmation of PCR amplification of the primers before PCR integration of 3XFLAG tag.

The primers confirmed by agarose gel electrophoresis were extracted from the gel and purified. The PCR product was used as the primers of the second PCR which is for the integration of FLAG tag into pENTR1A-NLRP13 plasmid. For the second PCR product, DpnI digestion was performed to cut the methylated sites and degrade

the leftover parental plasmid DNA. After the digestion, the product was transformed into Top10 strain of *E. coli* and grown on LB agar plates with kanamycin. On the next day, on the control group without DpnI enzyme, the plate seemed like a smear, and the experiment group had lots of colonies. 6 of the colonies were picked and the plasmid purification was performed. The analytical digestion of the plasmids was implemented with the EcoRV and the SacI enzymes and the product was run on 1% agarose gel. The expected band size for the short fragment was 517 bp for the template plasmid and 595 bp for the pENTR1A-NLRP13-FLAG plasmid. 5 of the 6 colonies had a band at 595 bp (Figure 5.3). Colony 2 and 3 were confirmed via Sanger sequencing performed by Macrogen.

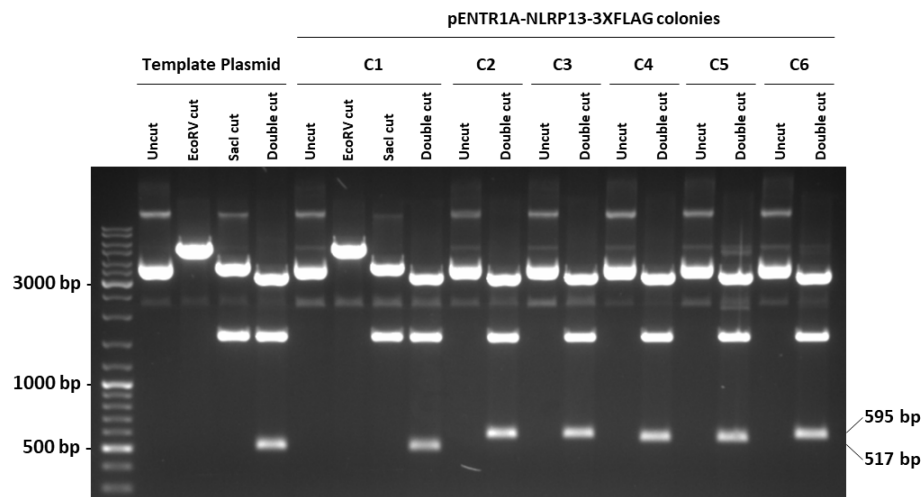


Figure 5.3. Analytical digestion of PCR integration colonies with EcoRV and SacI restriction digestion enzymes after DpnI digestion.

To generate THP-1 cell line stably overexpressing NLRP13-FLAG, the cloning of the NLRP13-3XFLAG sequence into pLEX307 ccdB plasmid was aimed via Gateway cloning. Prior to the Gateway cloning, the pENTR1A-NLRP13-FLAG vector was linearized by NheI restriction enzyme to facilitate cloning the sequence. The product was run on 1% agarose gel. The plasmid length of pENTR1A-NLRP13-FLAG is 5502 bp. The linear plasmid has been seen to shift up because of its linear form when compared to uncut control (Figure 5.4).

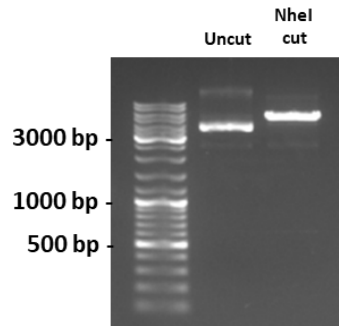


Figure 5.4. Linearization of pENTR1A-NLRP13-FLAG plasmid with NheI restriction digestion enzyme.

After the confirmation of the pENTR1A-NLRP13-FLAG plasmids via sequencing, and linearization of the plasmid, NLRP13-3XFLAG sequence was cloned to pLEX307 ccdB lentiviral expression vector by gateway cloning using Gateway™ LR Clonase™ II Plus Enzyme Mix. The reaction without LR Clonase™ was the negative control. After the gateway cloning, the product was transformed into Stbl3 strain of *E. coli* and grown on LB agar plates with ampicillin. On the next day, the experiment group had 9 colonies. All of the colonies were picked and the plasmid purification was performed. The plasmid concentrations of 2 colonies were not enough to analyze. 7 colonies were digested with BamHI enzyme to analyze and the product was run on 1% agarose gel. 3 bands, especially the band at 2947 bp, were expected for pLEX307-NLRP13-FLAG plasmid compared to the template plasmid which had 2 bands. All of the pLEX307-NLRP13-FLAG colonies had proper bands (Figure 5.5). These plasmids were validated not to contain SNPs or frameshifts via Sanger sequencing performed by MacroGen (Figure 5.6).

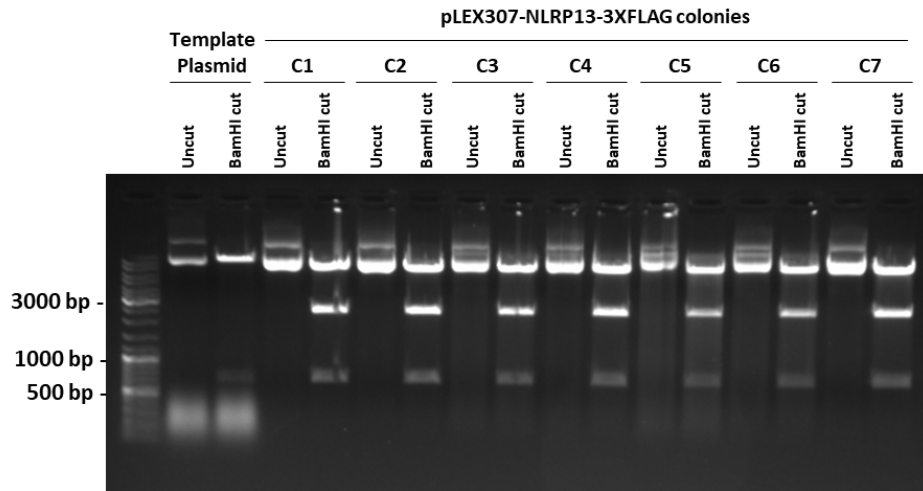


Figure 5.5. Analytical digestion of pLEX307-NLRP13-FLAG colonies with BamHI restriction enzyme.

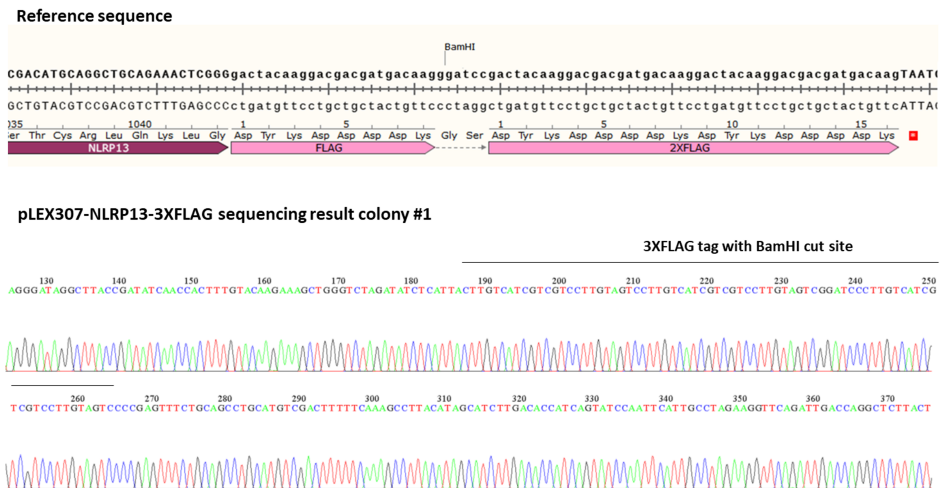


Figure 5.6. An electropherogram of Sanger sequencing of one of the pLEX307-NLRP13-FLAG plasmids obtained from the colonies along with a representation of the reference sequence of the region containing 3XFLAG tag.

After the cloning, to validate the protein expressions of NLRP13 and FLAG tag, the plasmids were transfected to HEK293FT cells via the Calcium Phosphate method. The cells collected after 48 hours were lysed and run on 12% SDS-PAGE gel and visualized via Western blotting. The lysate of pcDNA3-NLRP13-FLAG plasmid

was used as the positive control and the nontransfected cell lysate as the negative control. The calculated molecular weight of NLRP13-3XFLAG is 122 kDa. The protein expression of NLRP13 protein and FLAG tag was verified for 2 out of the 7 colonies via polyclonal rabbit anti-NLRP13 (Abcam, UK) and monoclonal mouse anti-FLAG(M2) (Sigma-Aldrich, Germany) antibodies (Figure 5.7).

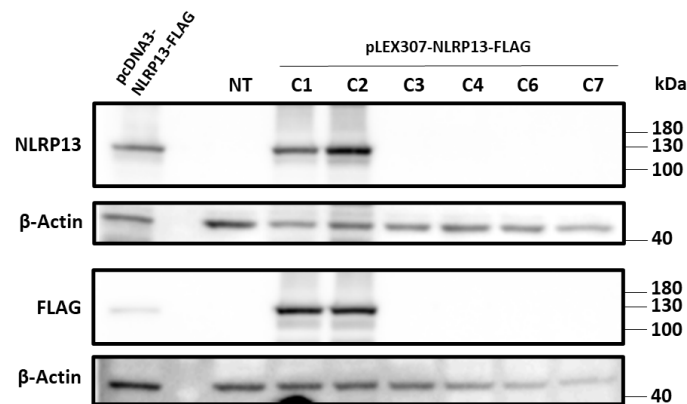


Figure 5.7. Validation of NLRP13 and 3XFLAG tag protein expressions of pLEX307-NLRP13-FLAG plasmids via Western blotting using anti-NLRP13 rabbit pAb, anti-FLAG mouse mAb and anti- β -Actin rabbit mAb. NLRP13-3XFLAG: 122 kDa, β -Actin: 42 kDa.

5.2.2. Transduction of THP-1 and Tera-2 cells and validation of NLRP13-FLAG expression levels

To generate NLRP13-FLAG-stable cell lines, NLRP13-FLAG-containing lentivirus production was performed. Firstly, 3×10^6 HEK293FT cells were seeded into a 10-cm cell culture plate. After 48 hours, when the confluency was about 75-80%, the pCMV-VSV-g envelope plasmid, pCMV delta R8.2 packaging plasmid, and the expression plasmid (pLEX-GFP, -NLRP13, or -NLRP13-FLAG) were co-transfected to HEK293FT cells. The transfection efficiency was visualized under a fluorescent microscope via pLEX-GFP transfected cells (Figure 5.8).

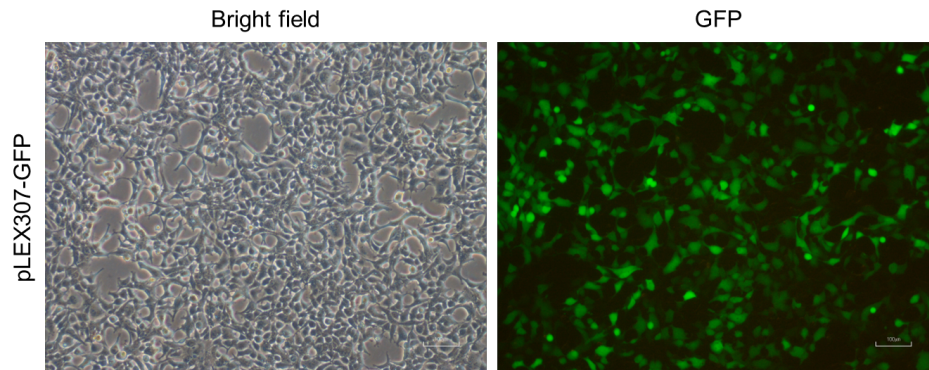


Figure 5.8. Transfection efficiency of HEK293FT cells transfected with pLEX plasmids and the packing plasmids for lentivirus production.

For transduction, at 48 hours after transfection, the NLRP13-FLAG-containing lentiviruses were harvested, and 1×10^6 THP-1 cells were transduced. After 24 hours, the virus-containing medium was changed to fresh medium. On the third day of infection, puromycin selection was started for the selection of the transduced cells and continued until all the non-transduced cells were dead (Figure 5.9a). After 48 hours of transduction, the transduction efficiency was visualized under a fluorescent microscope via pLEX-GFP-stable THP-1 cells (Figure 5.9b). To analyze the efficiency of transduction, flow cytometry was performed with 200,000 THP-1-GFP cells after 3 days of puromycin selection. THP-1 WT cells were used as negative control. Gating strategy, which is sketching a region around the cell population of interest, was firstly on THP-1 WT cells, and then to THP-1 GFP+ cells. 99.8% of the cells were THP-1 GFP+ (Figure 5.9c).

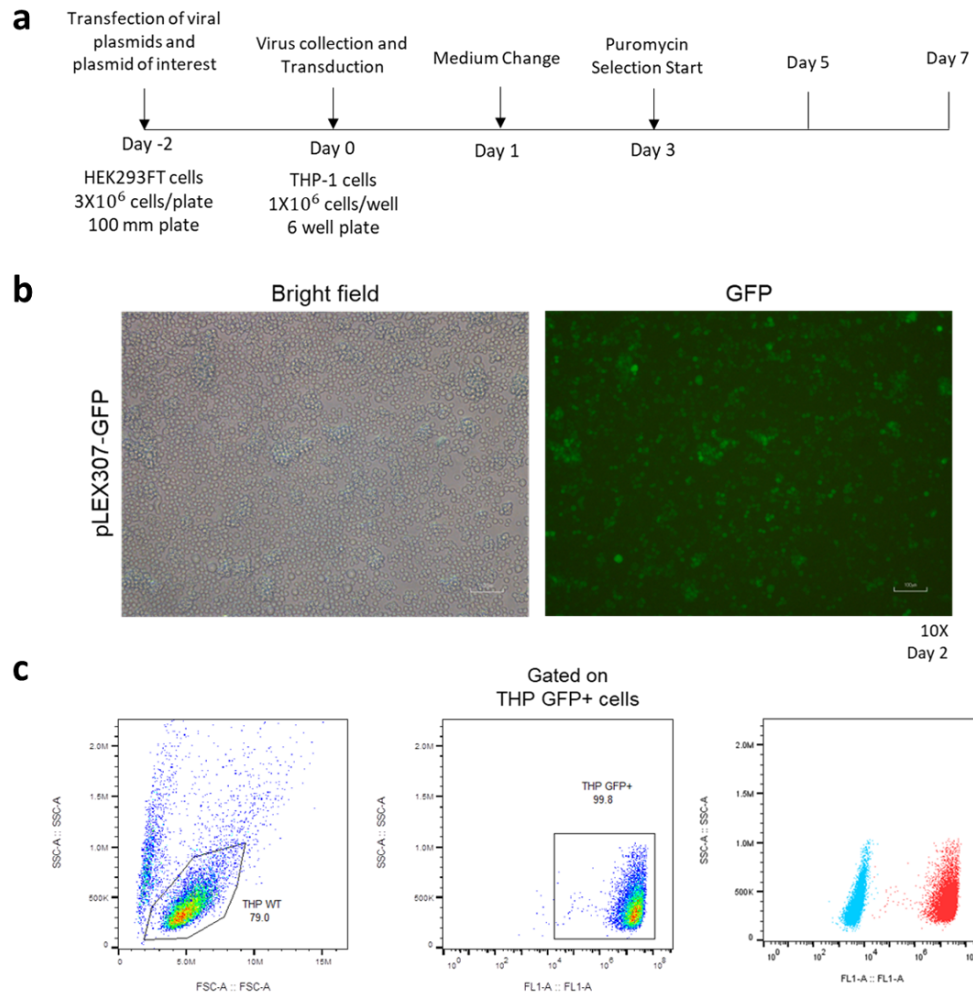


Figure 5.9. Transduction of THP-1 cells. (a) Schematic representation of the experimental procedure for transduction of THP-1 cells. (b) Lentiviral transduction efficiency visualized under a fluorescent microscope. (c) Lentiviral transduction efficiency detected via flow cytometry presenting the percentage of THP-1 GFP+ cells after puromycin selection. FSC-A, forward scatter-area; SSC-A, side scatter-area; FL1-A, fluorescence detector for GFP.

For Tera-2 cells, 6×10^5 Tera-2 cells were seeded on 6-well cell culture plate. When the confluency was about 80-85%, the cells were infected with the NLRP13-FLAG-containing lentiviruses harvested previously after adding polybrene. After 24 hours, the virus-containing medium was changed to fresh medium. On the fifth day of infection, puromycin selection was started for the selection of the transduced cells and

continued until all the non-transduced cells were dead (Figure 5.10a). After 72 hours of transduction, the transduction efficiency was visualized under a fluorescent microscope via Tera-2-GFP cells (Figure 5.10b), and flow cytometry was performed with 200,000 Tera-2-GFP cells. Tera-2 WT cells were used as negative control. Gating strategy was firstly on Tera-2 WT cells, and then to Tera-2 GFP+ cells. 86.7% of the cells were Tera-2 GFP+ (Figure 5.10c).

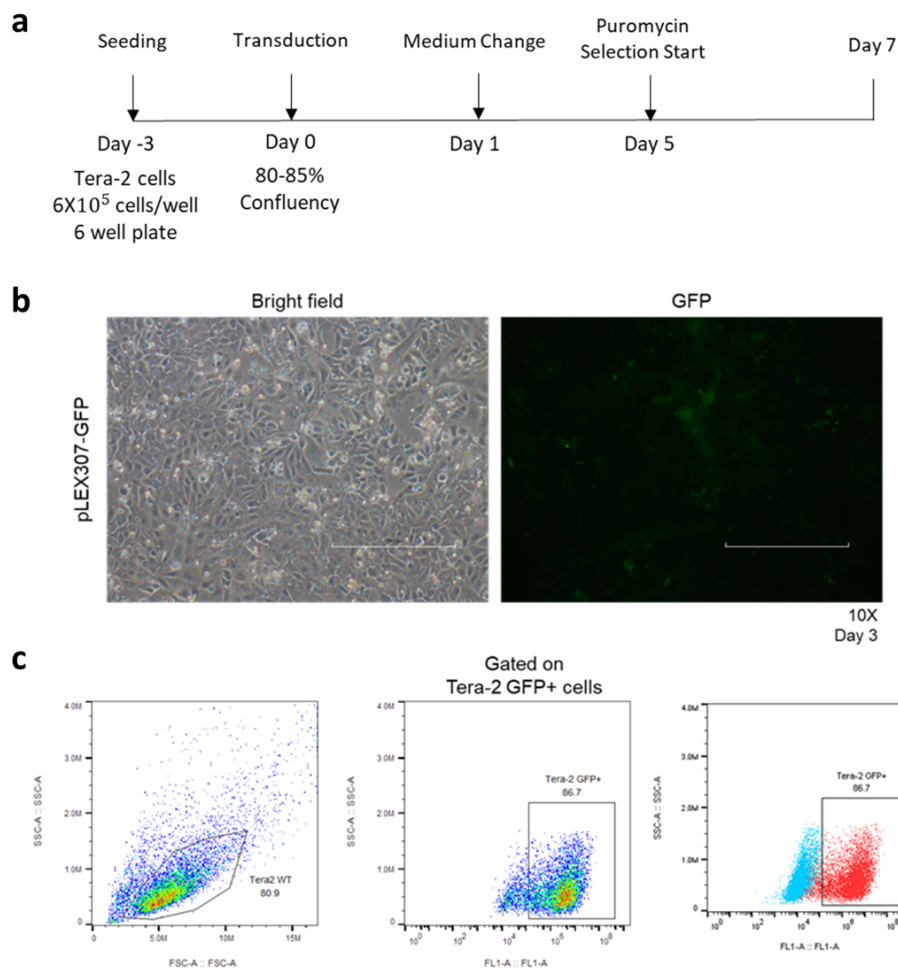


Figure 5.10. Transduction of Tera-2 cells. (a) Schematic representation of the experimental procedure for transduction of Tera-2 cells. (b) Lentiviral transduction efficiency visualized under a fluorescent microscope. (c) Lentiviral transduction efficiency detected via flow cytometry presenting the percentage of Tera-2 GFP+ cells on day 3 after transduction. FSC-A, forward scatter-area; SSC-A, side scatter-area; FL1-A, fluorescence detector for GFP.

The protein expression levels of THP-1 stably overexpressing NLRP13-FLAG cells were controlled. 1×10^6 THP-1-GFP, -NLRP13, -NLRP13-FLAG cells were counted and collected. The cell lysates were on 12% SDS-PAGE gel and visualized via Western blotting for both NLRP13 protein and FLAG tag. The lysate of pcDNA3-NLRP13-FLAG plasmid was used as the positive control. The protein bands at 122 kDa were detected in NLRP13-FLAG-stable THP-1 cells while the band for THP-1-NLRP13 was at 119 kDa, and no band for THP-1-GFP cells. For both plasmids isolated from the colonies, NLRP13 and FLAG expressions were confirmed in NLRP13-FLAG-stable THP-1 cells compared to controls (Figure 5.11).

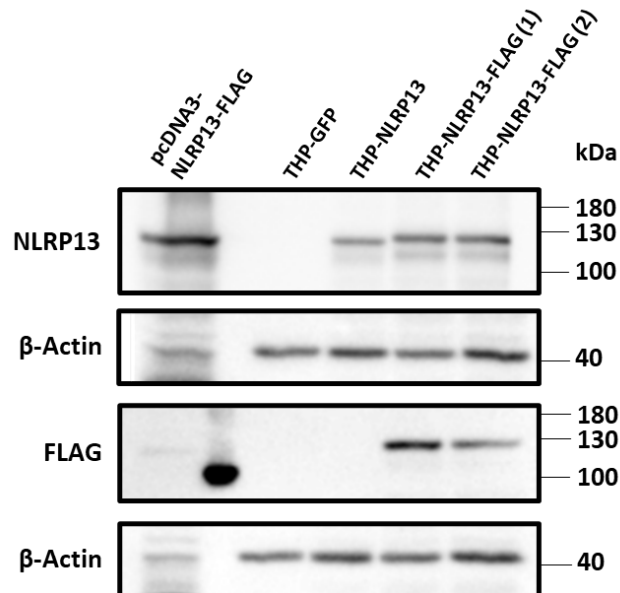


Figure 5.11. Validation of protein expression in NLRP13-FLAG-stable THP-1 cells via Western blotting by using anti-NLRP13 rabbit pAb and anti-FLAG mouse mAb.

NLRP13-3XFLAG: 122 kDa, β -Actin: 42 kDa.

NLRP13-FLAG protein expression levels were also controlled in NLRP13-FLAG-stable Tera-2 cells. 1×10^6 Tera-2-WT, -GFP, and -NLRP13-FLAG cells were counted and collected. The cell lysates were run on 12% SDS-PAGE gel and visualized via Western blotting for both NLRP13 protein and FLAG tag. The lysate of pcDNA3-NLRP13-FLAG plasmid was used as the positive control. THP-1-NLRP13 lysate was the other control for checking the level of NLRP13 band. Tera-2 WT and Tera-2-

GFP cells were the negative controls. NLRP13-FLAG-stable Tera-2 cells showed both NLRP13 and FLAG expression at the correct level compared to controls (Figure 5.12).

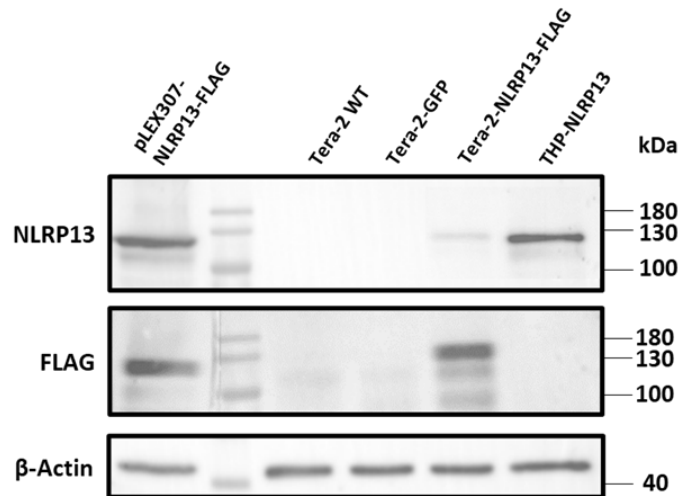


Figure 5.12. Validation of protein expression in NLRP13-FLAG-stable Tera-2 cells via Western blotting by using anti-NLRP13 rabbit pAb and anti-FLAG mouse mAb. NLRP13-3XFLAG: 122 kDa, β -Actin: 42 kDa.

5.3. Investigation of Interaction Partners of NLRP13

5.3.1. Co-immunoprecipitation of NLRP13 via FLAG antibody

NLRP13 was co-immunoprecipitated from NLRP13-FLAG-stable THP-1 cells by using monoclonal anti-FLAG antibody. The co-immunoprecipitation (co-IP) using mouse IgG antibody was the negative control. In the first trial, 15×10^6 cells were used for total protein lysate. 50 μ l of beads were incubated with 5 μ g of FLAG mAb. For the analysis, the samples from wash steps were also collected. The beads were eluted directly with 2X Laemmli buffer. The co-IP elutions were run on 12% SDS-PAGE gel. To confirm that co-IP was working, the proteins were visualized via Coomassie Blue staining and Western blotting. In Coomassie Blue staining, the bands of the heavy and light chains of the antibody were slightly seen at 25 and 50 kDa. However, the NLRP13 band was not clear (Figure 5.13a). In Western blot analysis, NLRP13 band was clearly detected, and the band was absent in the mouse IgG control sample (Figure

5.13b). WCL and FT samples had a weaker band for NLRP13 than the eluted sample, as well. The co-IP trial was successfully performed, however, the number of cells and the elution method needed to be improved.

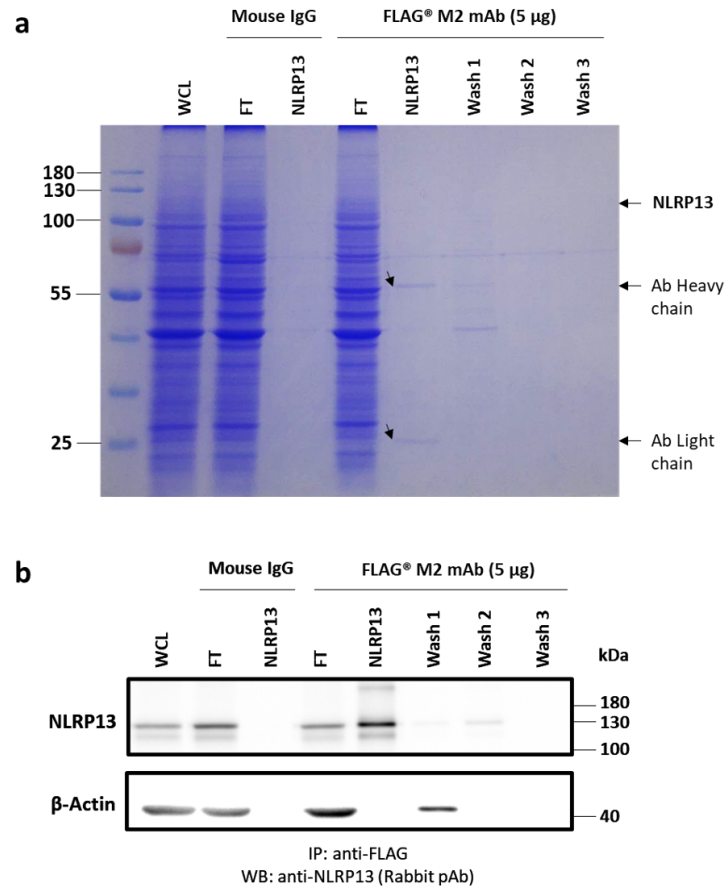


Figure 5.13. Co-immunoprecipitation of NLRP13 eluted with Laemmli buffer. (a) Coomassie Blue Staining. WCL, whole cell lysate; FT, flow-through. (b) Western blotting using anti-NLRP13 rabbit pAb and anti- β -Actin rabbit mAb. IP was performed with anti-FLAG mouse mAb. NLRP13-3XFLAG: 122 kDa, β -Actin: 42 kDa.

Since the elution of NLRP13 was not clearly observed in Coomassie Blue staining, co-IP experiment was repeated with a higher number of NLRP13-FLAG-stable THP-1 cells. 22.5×10^6 cells were lysed and co-IP experiment was repeated. As a technical optimization, FLAG antibody was firstly incubated with beads or lysate and put overnight incubation after adding lysate or transferring into beads, respectively, to observe if

any difference between the pre-immobilized antibody or free antibody approaches for the attachment of the antibody and the amount of pull-down NLRP13. In Coomassie staining, the bands of the heavy and light chains of the antibody were seen at 25 and 55 kDa. NLRP13 was not clearly seen, again (Figure 5.14a). However, in Western blot analysis, NLRP13 was clearly detected, and the band was absent in the IgG control sample (Figure 5.13b). Any difference for the amount of eluted NLRP13 was not observed in the samples that the conjunction of the FLAG antibody was performed firstly with beads or lysate (Figure 5.14b). The next co-IP experiments were continued with the incubation of the antibody and beads prior to adding lysate.

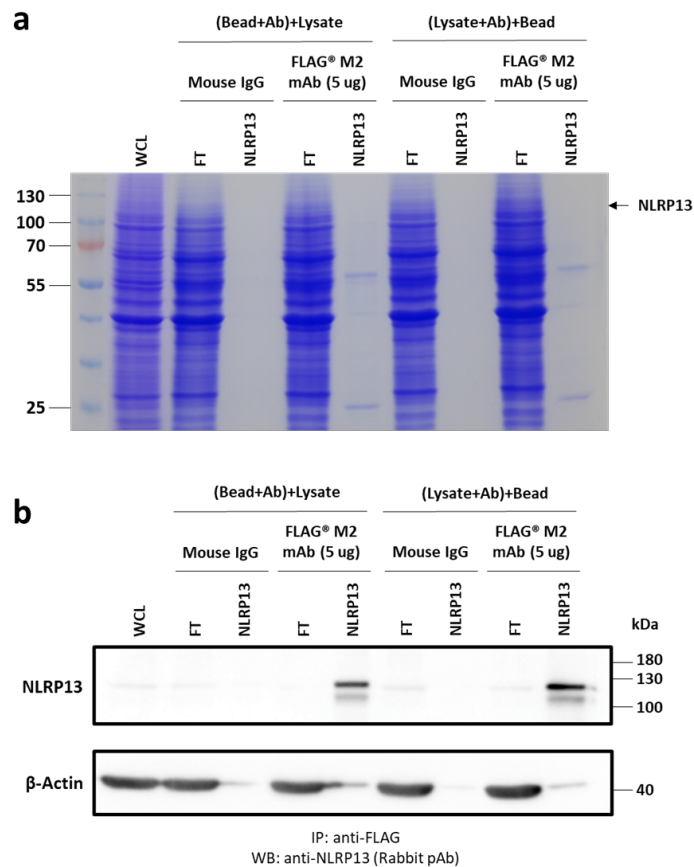


Figure 5.14. Optimization of co-immunoprecipitation of NLRP13 eluted with Laemmli buffer. (a) Coomassie Blue Staining. WCL, whole cell lysate; FT, flow-through. (b) NLRP13 was detected by anti-NLRP13 rabbit pAb via WB. IP was performed with anti-FLAG mouse mAb. NLRP13-3XFLAG: 122 kDa, β -Actin: 42 kDa.

To optimise the setting for observation of NLRP13 in SDS-PAGE gel, the number of cells lysed was increased to 30×10^6 . For the elution, glycine buffer and Laemmli buffer were used. 50 μ l of glycine buffer was added to the bead after the last wash and incubated for 10 minutes. The supernatant was collected. 5 μ l of neutralization buffer was added to the supernatant before the analysis (NLRP13 1.1). In addition, after collecting the supernatant, the beads were eluted once more with 2X Laemmli buffer and 0.2% NP-40 lysis buffer in 1:1 ratio to observe if NLRP13 was completely eluted (NLRP13 1.2). Another co-IP sample was directly eluted with 2X Laemmli buffer and lysis buffer as mentioned above (NLRP13 2). The negative control was the sample only eluted with glycine buffer. In Coomassie staining, a slight band for NLRP13 was observed at 122 kDa for all the experiment samples, and it was not observed in negative control (Figure 5.15). The antibody chains were observed at 25 and 55 kDa, as well. NLRP13 1.1 sample had weaker antibody bands than the Laemmli elutes.

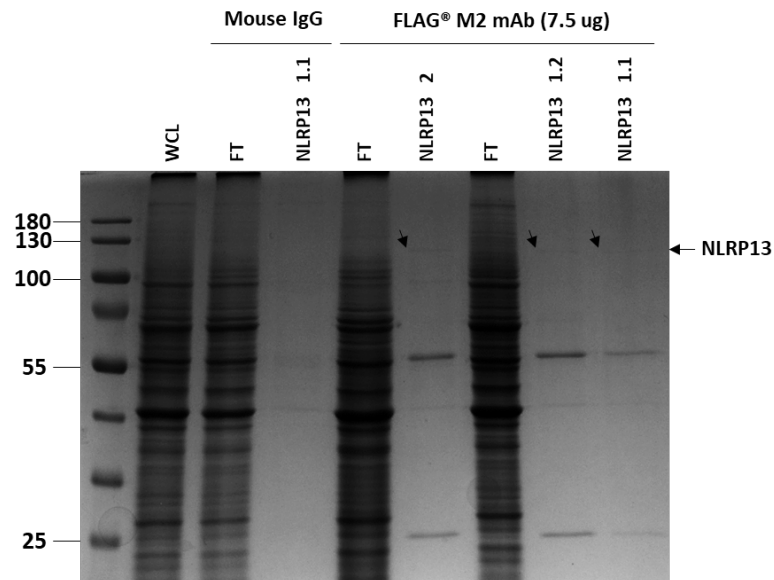


Figure 5.15. Co-immunoprecipitation samples eluted with glycine buffer were visualized via Coomassie Blue staining. WCL, whole cell lysate; FT, flow-through.

The protein levels of NLRP13 of glycine elution samples were analyzed by Western blotting. NLRP13 was clearly detected at 122 kDa (Figure 5.16). The negative control also had a weak band that might be because of insufficient washing.

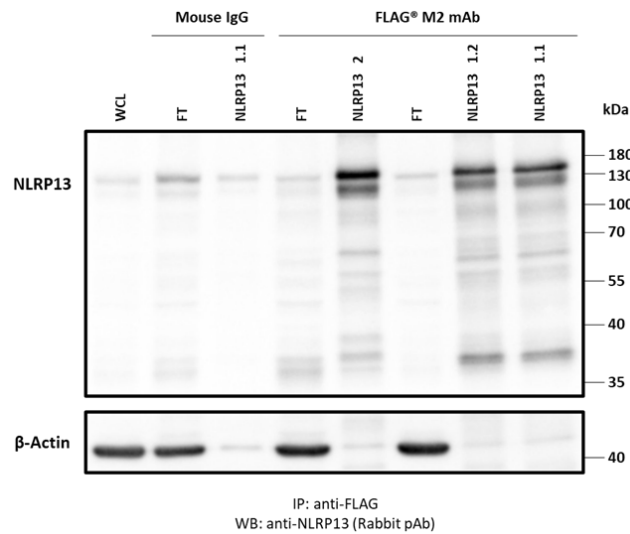


Figure 5.16. Co-immunoprecipitation samples eluted with glycine buffer were detected by anti-NLRP13 rabbit pAb and anti- β -Actin rabbit mAb via Western blotting. IP was performed with anti-FLAG mouse mAb. NLRP13-3XFLAG: 122 kDa, β -Actin: 42 kDa.

For the mass spectrometry, at least 2-3 mg of total protein is supposed to be used in immunoprecipitation. To determine the protein concentration, PierceTM BCA Protein Assay Kit (Thermo Fisher Scientific, USA) was performed (data not shown) and the concentration of 30×10^6 NLRP13-FLAG-stable THP-1 cells was calculated as 1816.9 $\mu\text{g}/\text{ml}$. So that, for 2.5 mg of total protein, the number of cells needed for immunoprecipitation was determined as 40×10^6 cells.

NLRP13 was co-immunoprecipitated from NLRP13-FLAG-stable THP-1 cells by using monoclonal FLAG antibody. The co-IP using mouse IgG antibody was the negative control. The beads were firstly eluted with 7M urea (NLRP13 1.1), and then, eluted with Laemmli (NLRP13 1.2) to ensure that all the proteins were eluted. The IP elutions were run on 12% SDS-PAGE gel. To confirm that co-IP was working, the proteins were visualized via Coomassie Blue staining and Western blotting. In Coomassie Blue staining, the bands of the heavy and light chain of the antibody were slightly seen at 25 and 55 kDa. However, the NLRP13 band was not clear (Figure 5.17).

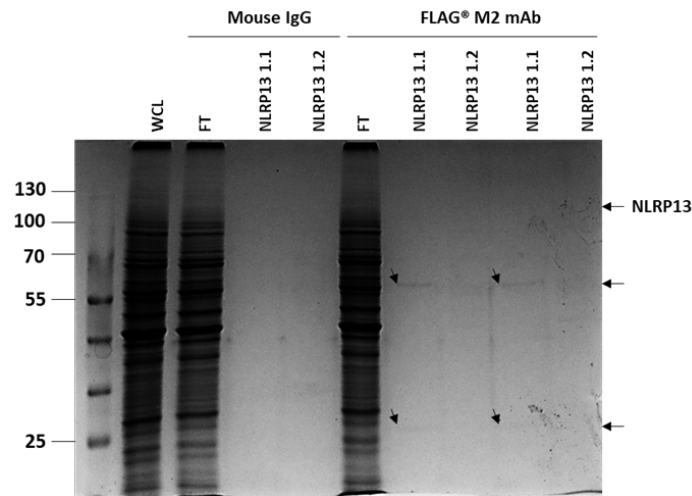


Figure 5.17. Co-immunoprecipitation samples eluted with urea buffer were visualized via Coomassie Blue staining. WCL, whole cell lysate; FT, flow-through.

Urea elution is the preferred method for the samples that will be analyzed in mass spectrometry. In the Western blot analysis, NLRP13 bands were clearly detected, and the band was absent in the IgG control sample (Figure 5.18). However, the difference between NLRP13 1.1 and 1.2 bands demonstrates that most of the proteins may be still bound to beads after urea elution. Still, the samples were sent to mass spectrometry. However, the results were not sufficient to provide a clue in finding the signaling pathways and molecular functions of NLRP13 (Figure 5.22).

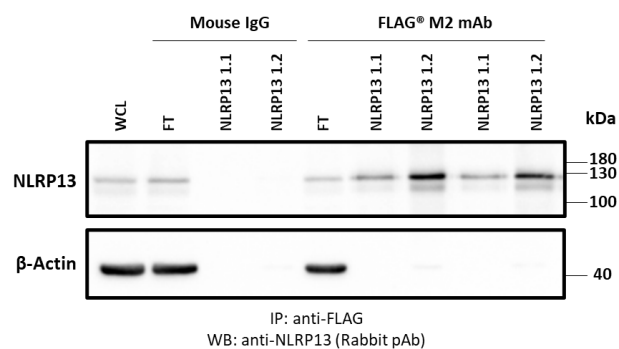


Figure 5.18. Co-immunoprecipitation samples eluted with urea buffer were detected by anti-NLRP13 rabbit pAb and anti- β -Actin rabbit mAb via WB. IP was performed with anti-FLAG mouse mAb. NLRP13-3XFLAG: 122 kDa, β -Actin: 42 kDa.

Thereafter, NLRP13-FLAG-stable THP-1 cells under the inflammasome activation condition and NLRP13-FLAG-stable Tera-2 cells were included to the experiment in which NLRP13's interaction partners were investigated, as well. Prior to this, the protein expression levels were checked in PMA-differentiated or undifferentiated THP-1 cells overexpressing NLRP13-FLAG primed with LPS incubated different durations and activated with ATP to obtain higher amount of protein yield in immunoprecipitation (Figure 5.19). 2.5×10^6 cells were used for PMA differentiation and expected to yield 1×10^6 cells while collecting, in addition, 1×10^6 cells were used for THP-1 monocytes (Figure 5.19a). In undifferentiated THP-1 cells, 3- or 6-hour LPS incubation followed by ATP treatment slightly upregulated NLRP13 expression and it did not represent any difference between 3-hour and 6-hour LPS treatment. In PMA-differentiated THP-1 cells, LPS/ATP treatment did not lead to a significant change in NLRP13 levels in overall, but 6-hour LPS stimulation led to a slight extent. Considering the actin levels, NLRP13 was observed less expressed in PMA-differentiated cells than undifferentiated monocytic cells (Figure 5.19b).

Judging also from previous studies in the lab, immunoprecipitation was performed with PMA-differentiated THP-1 cells overexpressing NLRP13-FLAG primed with LPS for 6 hours and activated with ATP.

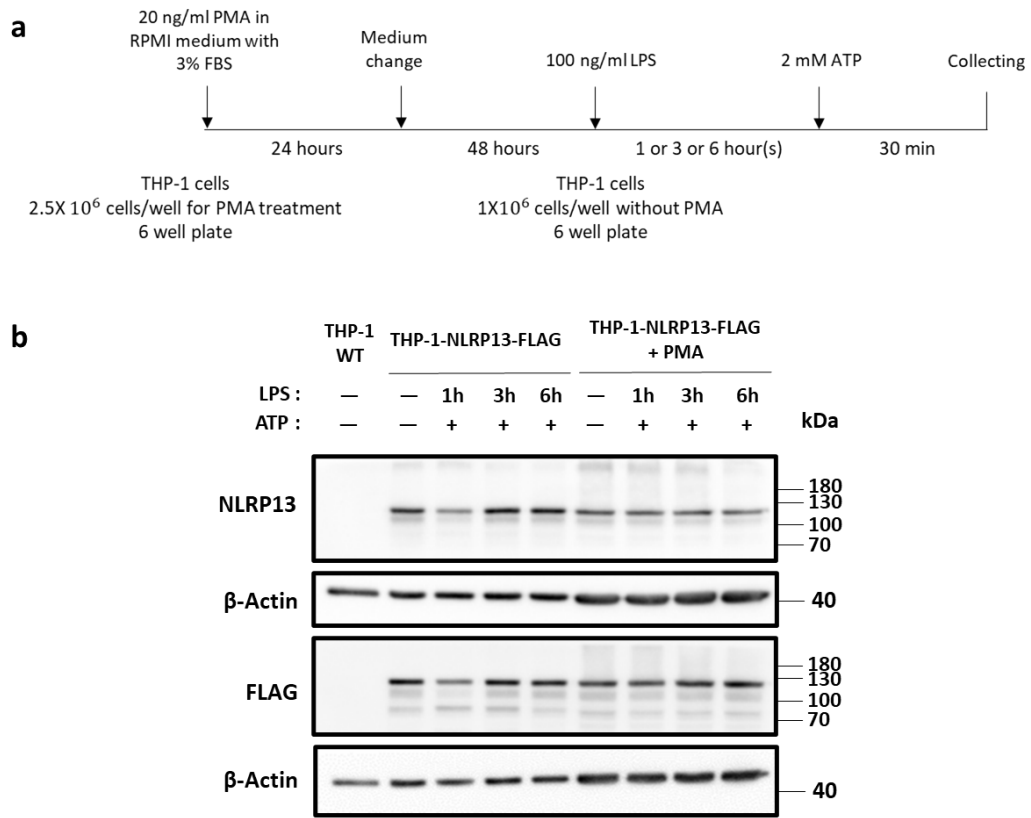


Figure 5.19. Protein expression levels in NLRP13-FLAG-stable THP-1 cells with or without PMA differentiation upon LPS/ATP treatment in a time-dependent manner. (a) Schematic representation of the experimental procedure. (b) NLRP13 and FLAG protein expression levels detected via Western blotting.

NLRP13 was also co-immunoprecipitated from 2.5x10⁶ of NLRP13-FLAG-stable THP-1 macrophages treated with LPS/ATP and NLRP13-FLAG-stable Tera-2 cells by using monoclonal anti-FLAG antibody. The beads were eluted with 2X Laemmli and run on 12% SDS-PAGE gel. To confirm that NLRP13 was pulled-down, the samples were visualized via Coomassie Blue staining and Western blotting. In Coomassie Blue staining, NLRP13 band from the immunoprecipitate of THP-1 macrophages could be observed on gel while there was no band on negative control. However, the NLRP13 band from the immunoprecipitate of Tera-2 cells was not clearly determined (Figure 5.20).

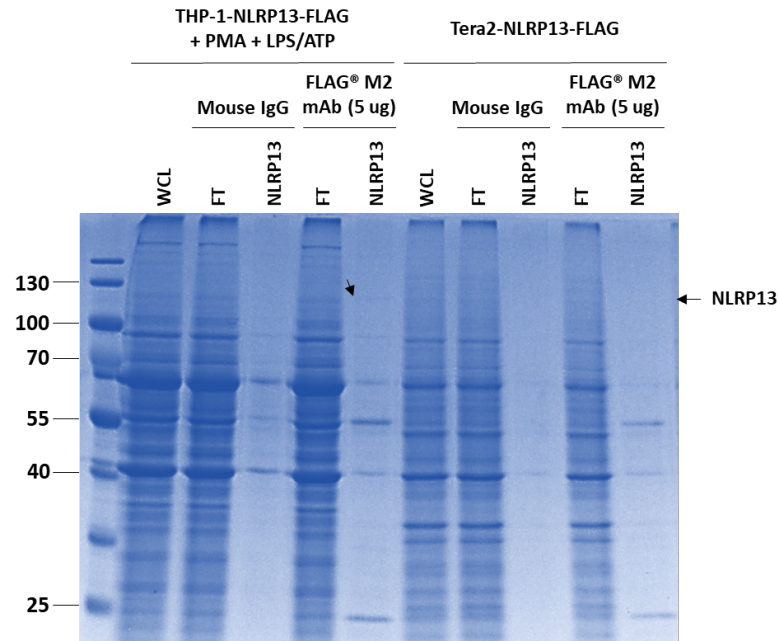


Figure 5.20. Co-immunoprecipitation of NLRP13 from THP-1-NLRP13-FLAG macrophages and Tera-2-NLRP13-FLAG cells by anti-FLAG antibody visualized via Coomassie Blue staining. Anti-FLAG immunoprecipitates from cell lysates were eluted with Laemmli buffer. WCL, whole cell lysate; FT, flow-through.

NLRP13 immunoprecipitated by anti-FLAG antibody was detected both in the samples of primed and ATP-activated THP-1 macrophages and that of Tera-2 cells by polyclonal anti-NLRP13 antibody via Western blotting (Figure 5.21). The amount of NLRP13 from Tera-2 cells was much weaker compared to THP-1 macrophages despite of considering the difference between actin levels (Figure 5.21b).

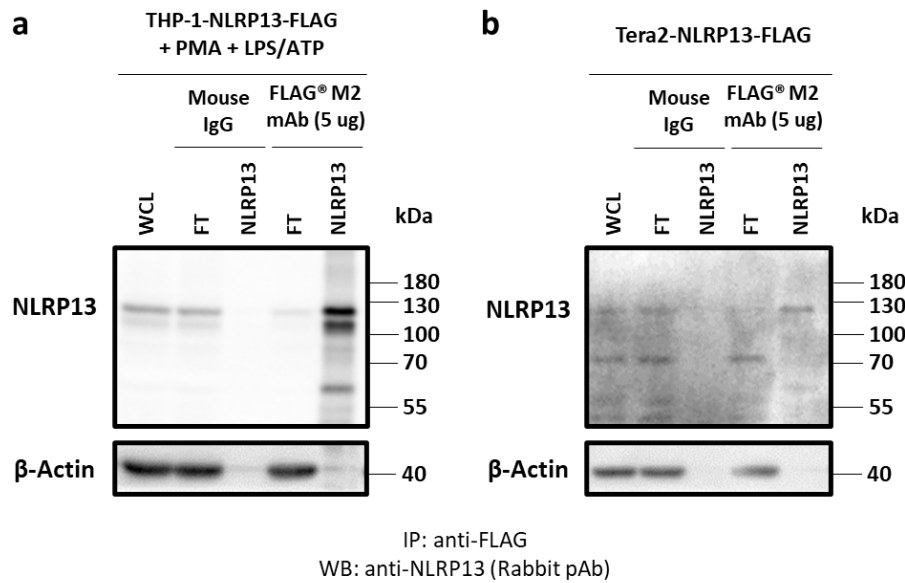


Figure 5.21. Co-immunoprecipitation of NLRP13 from THP-1-NLRP13-FLAG macrophages and Tera-2-NLRP13-FLAG cells by anti-FLAG antibody analyzed via Western blotting. Anti-FLAG immunoprecipitates from cell lysates were eluted with Laemmli buffer. (a) Co-IP of NLRP13 with immobilized anti-FLAG antibodies using WCL from THP-1-NLRP13-FLAG macrophages upon LPS/ATP treatment. (b) Co-IP of NLRP13 with immobilized anti-FLAG antibodies using WCL from Tera-2-NLRP13-FLAG cells.

To analyze interaction partners of NLRP13 in different concepts via mass spectrometry, three experiment groups with their biological duplicates, 40×10^6 of NLRP13-FLAG-stable THP-1 cells, 5×10^6 of NLRP13-FLAG-stable THP-1 macrophages with LPS/ATP treatment and 5×10^6 of NLRP13-FLAG-stable Tera-2 cells, were used in co-IP. For mass spectrometry analysis, it was supposed to have at least 1 mg of total protein to use in co-IP. Hence, the protein concentrations was determined via Pierce™ BCA Protein Assay Kit (Thermo Fisher Scientific, USA)(data not shown). The concentrations were calculated as $1764.34 \mu\text{g/ml}$ for 40×10^6 NLRP13-FLAG-stable THP-1 cells, $1588.32 \mu\text{g/ml}$ for 5×10^6 LPS/ATP-treated NLRP13-FLAG-stable THP-1 macrophages, and $1740.37 \mu\text{g/ml}$ for 5×10^6 NLRP13-FLAG-stable Tera-2 cells. According to these results, the amounts of total protein lysates varied between 1.5-1.8 mg. The samples of these three groups were eluted with Laemmli buffer and 80% of each

elute were run on SDS-PAGE gel. The proteins were eluted from gel matrix and sent mass spectrometry for the analysis.

5.3.2. Bioinformatic Analysis of NLRP13 Interaction Partners Using Mass Spectrometry Data

The most expected result from mass spectrometry was to detect a high number of peptides for NLRP13 and the other proteins with lower number of specific peptides, which should be absent in the control IgG group. If so, they may be considered as the potential interaction partners of NLRP13. In the mass analysis, the peaks were very weak and no NLRP13 peptides could be detected. A few peptides from the other proteins were detected with a low coverage rate, however, overall, the results of the mass analysis were not reasonable to identify the interaction partners of NLRP13 (Figure 5.22).

Protein Description	Accession	Gene	mW (kDa)	pI (pH)	PLGS score	Peptides	Theoretical peptides	Coverage (%)
T cell receptor alpha joining 56	A0A075B6Z2	TRAJ56	2.22	10.71	1526.2	3	2	38.1
Immunoglobulin kappa variable 2D-30	A0A075B6S6	IGKV2D-30	13.2	8.23	854.4	2	6	32.5
RNA polymerase II subunit A C-terminal domain phosphatase SSU72	A0A1W2PQJ5	SSU72P3	22.4	4.99	306.1	3	14	31.95
Zinc finger and SCAN domain-containing protein 30	Q86W11	ZSCAN30	56.3	6.23	278	8	49	24.1
Splicing regulatory glutamine/lysine-rich protein 1	Q8WXA9	SREK1	59.3	10.87	310.6	22	328	42.5

Figure 5.22. Mass spectrometry analysis of NLRP13-FLAG immunoprecipitation using anti-FLAG antibody.

Due to various glitches, the results of repeated experiments could not be reached yet. However, the analysis of the obtained immunoprecipitates for NLRP13-FLAG-stable THP-1 monocytes, LPS/ATP-treated NLRP13-FLAG-stable THP-1 macrophages and NLRP13-FLAG-stable Tera-2 cells continues.

6. CONCLUSION AND DISCUSSION

As all proteins, NLRs are crucial players in a dynamic network. Currently, NLRP13 is still an uncharacterized member of NLR family. Previously in our lab, various leading outcomes were revealed such as its localization, association with inflammasome components, upstream regulators, relation to cytokine secretion, cleavage by certain caspases and its potential role in cell death. NLRP13 is mainly in the cytoplasm and conceivably in mitochondria. It also weakly interacts with inflammasome components, ASC and Caspase-1, but not with Caspase-5. Additionally, it was shown that NLRP13 forms inflammasome-like structures with ASC and Caspase 1 [28]. NLRP13 protein expression is decreased when it is co-transfected with Caspase 8 or 9, the initiator caspases of extrinsic and intrinsic apoptotic pathways, respectively, in HEK293FT cells. Moreover, LPS and ATP are determined as the upstream regulators of NLRP13, and upon LPS/ATP treatment, NLRP13 leads to increase proIL-1 β and mature IL-1 β levels [29]. NLRP13 generates a *Pseudomonas aeruginosa*-specific innate immune response, and upon both LPS/ATP treatment and *P. aeruginosa* infection, the secretion levels of pro-inflammatory cytokines of NLRP13-stable THP-1 macrophages are increased compared to noninfected PMA-differentiated cells. In *in vitro* cleavage assay, NLRP13 shows a correlation with Caspase 8 [30]. NLRP13 is cleaved by Caspase-8 which is activated upon FADD recruitment following Fas ligand binding to Fas receptor, and the cleaved C-terminal of NLRP13 is partly localized to mitochondria [31]. It was also shown that NLRP13 does not have an effect on macrophage polarization in THP-1 macrophages [31]. In the view of cell death, it was shown that NLRP13 do not directly involve in pyroptosis via Caspase-8. However, PARP-1 cleavage, a hallmark of apoptosis, is decreased in NLRP13-stable THP-1 cells in which Caspase-8 is inhibited [32]. So, the results suggest NLRP13 could be involved in the molecular switch mechanism between apoptosis and pyroptosis via Caspase-8 activation complex [32].

The proteins interacting with NLRP13 are one of the uncharacterized features of NLRP13. Protein-protein interactions show substantial evidence to understand the

roles of proteins in biological processes. So that, with the purpose of identifying novel interaction partners of NLRP13, NLRP13-FLAG-stable cell lines were generated, and co-immunoprecipitation was performed followed by mass spectrometry. Initially, the endogenous expression levels of NLRP13 were determined in various human cell lines, including embryonal, placental, endometrial, and lymphocytic cell lines, under endogenous conditions. THP-1 and Tera-2 cell lines had endogenous NLRP13 expression at 119 kDa.

To maximize the potential interaction partners of NLRP13, the co-IP experiments were done under overexpression conditions, and FLAG tag was used for pull-down. FLAG-tagged NLRP13 was generated via PCR integration and Gateway cloning. 3X-FLAG tag was added to the C-terminus of NLRP13 protein in pENTR1A plasmid via PCR integration. After NLRP13-3XFLAG sequence in pENTR1A plasmid was confirmed, the sequence was successfully cloned into pLEX307 lentiviral plasmid via Gateway cloning. NLRP13-FLAG-expressing pLEX307 was used to generate stable cell lines. THP-1 and Tera-2 cells were infected with the lentiviruses containing the plasmid. The protein expressions of NLRP13 and FLAG was successfully validated in NLRP13-FLAG-stable THP-1 and Tera-2 cells.

Co-immunoprecipitation is a powerful biochemical method to identify the interaction partners. In co-IP, an antigen along with any proteins bound to it is isolated from a mixture via a specific antibody immobilized on a solid support. Firstly, NLRP13-FLAG-stable THP-1 cells were used for our co-IP experiments. The co-IP experiments of stable Tera-2 cell line could not be performed in the initial trials because of its slow growth rate. After co-IP of NLRP13 from THP-1 cells by monoclonal anti-FLAG antibody, the expected band was successfully observed in Western blot by using polyclonal anti-NLRP13 antibody. The co-IP experiments were repeated by increasing the number of cells, in other words, by increasing the total amount of protein used in the experiments, and also by using different elution methods to receive effective results for network analysis.

As the elution methods compatible with mass spectrometry, glycine elution and urea elution methods were tried other than the standard elution (Laemmli buffer) which is not compatible with mass spectrometry. Glycine buffer is used as a nondenaturing elution buffer with low pH conditions. The glycine elution provided an effective elution for NLRP13, however, the bands were still weak in Coomassie staining, even though NLRP13 could eventually be observed. In glycine elution, it was also seen antibody fragment contamination which was undesirable in mass spectrometry analysis. Lastly, urea buffer was used as denaturing buffer preferably used in the samples that will be analyzed in mass spectrometry. Urea disrupts hydrogen bonds in proteins and solubilizes everything, which provides a suitable environment for proteolytic cleavage before mass spectrometry.

The duplicated samples eluted with urea buffer were sent to mass spectrometry. However, the analysis result in that NLRP13 peptides could not be even detected. A few peptides from the other proteins were detected, but with a low coverage rate. Overall, the results of the first trial of mass spectrometry analysis to identify the interaction partners of NLRP13 did not provide a reasonable aspect to get information about its biological function and its role in signaling pathways.

After the adverse outcomes, the experiment groups were expanded, and NLRP13-FLAG-stable THP-1 cells under inflammasome activation condition and NLRP13-FLAG-stable Tera-2 cells were also included in the experiment to gain insight into the biological functions of NLRP13. Prior to this, the protein expression levels were checked in PMA-differentiated or undifferentiated THP-1 cells overexpressing NLRP13-FLAG primed with LPS incubated different durations and activated with ATP to obtain higher amount of protein yield in co-IP. Despite the fact that NLRP13 expression in PMA-differentiated cells was observed less than undifferentiated monocytes, which is in line with the previous results in lab, the effective inflammation activation and the advantage of increased cytoplasm and ribosome numbers in macrophages were led us to use PMA-differentiated LPS/ATP-treated THP-1 cells overexpressing NLRP13-FLAG in the subsequent experiments.

After additionally performing the co-IP experiments of stable THP-1 macrophages and stable Tera-2 cells, NLRP13 pull-down was confirmed via Coomassie Blue staining and Western blotting. NLRP13 yield from Tera-2 cells was notably weak in line with its relative weaker expression in Tera-2 cells than the THP-1 cells. In order to get the highest amount of all collected protein complexes from the beads, harsh elution was firstly performed with Laemmli and followed by protein elution from the SDS-PAGE gel matrix by using urea buffer which was also preferred at the initial trial of mass spectrometry.

The pulled-down NLRP13 from NLRP13-FLAG-stable THP-1 monocytes, LPS/ATP-treated NLRP13-FLAG-stable THP-1 macrophages and NLRP13-FLAG-stable Tera-2 cells obtained via co-IP with anti-FLAG antibody were sent to mass spectrometry. Due to various glitches, the results of repeated experiments could not be reached yet. However, the analysis of the obtained immunoprecipitates continues.

Protein-protein interactions (PPIs) have key roles in various biological processes in cells including transcription, protein synthesis and degradation, cell-cell adhesion, cell cycle progression, signal transduction, metabolic pathways, and developmental process. Uncovering PPIs is crucial to understand the roles of multi-protein complexes in disease states. A phylogenetic tree is one of the *in silico* methods to predict the PPIs of a protein. The phylogenetic analysis of the genes of the NLRP subfamily showed that NLRP13 is in the cluster of reproduction-related NLRPs including NLRP11/4/9/8/5/14 [17, 24, 33]. It is also known that NLRP13 is highly expressed in oocytes, and its expression decreases progressively in embryos with a very low level in day-5 embryos, similar to the other members of the cluster [24]. Tera-2 cell line is a human embryonal carcinoma cell line, and the immunoprecipitates obtained from the stable Tera-2 cells used in this study may point out potential interaction partners of NLRP13 in the concept of early development. THP-1 cell line is a human leukemia monocytic cell line that innately expresses PRRs, so that, it generates immune responses. NLRP13-FLAG stable THP-1 monocytes and LPS/ATP-treated THP-1 macrophages used in this study may indicate potential interactions of NLRP13 with inflammasome components such as ASC and Caspase-1. The study of Gebremicael

et al. in HIV and tuberculosis co-infected patients and the previous study in our lab about the partial localization of the cleaved C-terminal of NLRP13 to mitochondria may suggest that NLRP13 contributes to mitochondrial antiviral immune response or mitochondrial metabolic pathways [27, 31]. Overall, the prospective results of mass spectrometry analysis continuing may reveal the potential functions of NLRP13 in early embryonic development and innate immune defense.

In further studies, 3XFLAG peptide may be used as an alternative elution method of co-IP in which the pulled-down complexes are eluted from the beads by competition with 3X FLAG peptides. It provides the enrichment of protein complexes and prevents immunoglobulin elution. Reciprocal immunoprecipitation and immunoblotting should be performed to confirm the newly identified proteins which had a probability to be in interaction with NLRP13. It provides evidence that the identified protein is not a product of cross-reactivity or contamination. Additionally, Bio-ID method which includes proximity-dependent biotinylation can be applied to investigate the weak and/or transient interactions.

REFERENCES

1. Murphy, K. and C. Weaver, *Janeway's Immunobiology*, Ninth Edition, Garland Science, New York, 2016.
2. Castelo-Branco, C. and I. Soveral, "The Immune System and Aging: A Review", *Gynecological Endocrinology*, Vol. 30, No. 1, pp. 16–22, 2013.
3. Marshall, J. S., R. Warrington, W. Watson and H. L. Kim, "An Introduction to Immunology and Immunopathology", *Allergy, Asthma & Clinical Immunology*, Vol. 14, No. S2, p. 49, 2018.
4. Chaplin, D. D., "Overview of the Immune Response", *Journal of Allergy and Clinical Immunology*, Vol. 125, No. 2, pp. S3–S23, 2010.
5. Patel, S., "Danger-Associated Molecular Patterns (DAMPs): The Derivatives and Triggers of Inflammation", *Current Allergy and Asthma Reports*, Vol. 18, No. 11, p. 63, 2018.
6. Smith, N. C., M. L. Rise and S. L. Christian, "A Comparison of the Innate and Adaptive Immune Systems in Cartilaginous Fish, Ray-Finned Fish, and Lobe-Finned Fish", *Frontiers in Immunology*, Vol. 10, p. 2292, 2019.
7. Man, S. M. and B. J. Jenkins, "Context-Dependent Functions of Pattern Recognition Receptors in Cancer", *Nature Reviews Cancer*, Vol. 22, No. 7, pp. 397–413, 2022.
8. Saxena, M. and G. Yeretssian, "NOD-Like Receptors: Master Regulators of Inflammation and Cancer", *Frontiers in Immunology*, Vol. 5, p. 327, 2014.
9. Smith, S. and C. Jefferies, "Role of DNA/RNA Sensors and Contribution to Autoimmunity", *Cytokine & Growth Factor Reviews*, Vol. 25, No. 6, pp. 745–757,

2014.

10. Li, D. and M. Wu, “Pattern Recognition Receptors in Health and Diseases”, *Signal Transduction and Targeted Therapy*, Vol. 6, No. 1, p. 291, 2021.
11. Zhong, Y., A. Kinio and M. Saleh, “Functions of NOD-Like Receptors in Human Diseases”, *Frontiers in Immunology*, Vol. 4, p. 333, 2013.
12. Kim, Y. K., J.-S. Shin and M. H. Nahm, “NOD-Like Receptors in Infection, Immunity, and Diseases”, *Yonsei Medical Journal*, Vol. 57, No. 1, p. 5, 2016.
13. Steidl, C., S. P. Shah, B. W. Woolcock, L. Rui, M. Kawahara, P. Farinha, N. A. Johnson, Y. Zhao, A. Telenius, S. B. Neriah, A. McPherson, B. Meissner, U. C. Okoye, A. Diepstra, A. van den Berg, M. Sun, G. Leung, S. J. Jones, J. M. Connors, D. G. Huntsman, K. J. Savage, L. M. Rimsza, D. E. Horsman, L. M. Staudt, U. Steidl, M. A. Marra and R. D. Gascoyne, “MHC Class II Transactivator CIITA is a Recurrent Gene Fusion Partner in Lymphoid Cancers”, *Nature*, Vol. 471, No. 7338, pp. 377–381, 2011.
14. Ma, X., Y. Qiu, Y. Sun, L. Zhu, Y. Zhao, T. Li, Y. Lin, D. Ma, Z. Qin, C. Sun and L. Han, “NOD2 Inhibits Tumorigenesis and Increases Chemosensitivity of Hepatocellular Carcinoma by Targeting AMPK Pathway”, *Cell Death & Disease*, Vol. 11, No. 3, p. 174, 2020.
15. Gültekin, Y., E. Eren and N. Özören, “Overexpressed NLRC3 Acts as an Anti-Inflammatory Cytosolic Protein”, *Journal of Innate Immunity*, Vol. 7, No. 1, pp. 25–36, 2014.
16. Cummings, J. R. F., R. M. Cooney, G. Clarke, J. Beckly, A. Geremia, S. Pathan, L. Hancock, C. Guo, L. R. Cardon and D. P. Jewell, “The Genetics of NOD-Like Receptors in Crohn’s Disease”, *Tissue Antigens*, Vol. 76, No. 1, pp. 48–56, 2010.
17. Tian, X., G. Pascal and P. Monget, “Evolution and Functional Divergence of NLRP

- Genes in Mammalian Reproductive Systems”, *BMC Evolutionary Biology*, Vol. 9, No. 1, p. 202, 2009.
18. Peng, H., B. Chang, C. Lu, J. Su, Y. Wu, P. Lv, Y. Wang, J. Liu, B. Zhang, F. Quan, Z. Guo and Y. Zhang, “NLRP2, a Maternal Effect Gene Required for Early Embryonic Development in the Mouse”, *PLoS ONE*, Vol. 7, No. 1, p. e30344, 2012.
 19. Meyer, E., D. Lim, S. Pasha, L. J. Tee, F. Rahman, J. R. W. Yates, C. G. Woods, W. Reik and E. R. Maher, “Germline Mutation in NLRP2 (NALP2) in a Familial Imprinting Disorder (Beckwith-Wiedemann Syndrome)”, *PLoS Genetics*, Vol. 5, No. 3, p. e1000423, 2009.
 20. Tong, Z.-B., L. Gold, K. E. Pfeifer, H. Dorward, E. Lee, C. A. Bondy, J. Dean and L. M. Nelson, “Mater, a Maternal Effect Gene Required for Early Embryonic Development in Mice”, *Nature Genetics*, Vol. 26, No. 3, pp. 267–268, 2000.
 21. Gorp, H. V., A. Kuchmiy, F. V. Hauwermeiren and M. Lamkanfi, “NOD-Like Receptors Interfacing the Immune and Reproductive Systems”, *FEBS Journal*, Vol. 281, No. 20, pp. 4568–4582, 2014.
 22. Alici-Garipcan, A., B. Özçimen, İlke Süder, V. Ülker, T. T. Önder and N. Özören, “NLRP7 Plays a Functional Role in Regulating BMP4 Signaling During Differentiation of Patient-Derived Trophoblasts”, *Cell Death & Disease*, Vol. 11, No. 8, p. 658, 2020.
 23. Westerveld, G., C. Korver, A. van Pelt, N. Leschot, F. van der Veen, S. Repping and M. Lombardi, “Mutations in the Testis-specific NALP14 Gene in Men Suffering from Spermatogenic Failure”, *Human Reproduction*, Vol. 21, No. 12, pp. 3178–3184, 2006.
 24. Zhang, P., M. Dixon, M. Zucchelli, F. Hambiliki, L. Levkov, O. Hovatta and J. Kere, “Expression Analysis of the NLRP Gene Family Suggests a Role in Human

- Preimplantation Development”, *PLoS ONE*, Vol. 3, No. 7, p. e2755, 2008.
25. Chu, J.-Q., G. Shi, Y.-M. Fan, I.-W. Choi, G.-H. Cha, Y. Zhou, Y.-H. Lee and J.-H. Quan, “Production of IL-1 β and Inflammasome with Up-Regulated Expressions of NOD-Like Receptor Related Genes in *Toxoplasma gondii*-Infected THP-1 Macrophages”, *The Korean Journal of Parasitology*, Vol. 54, No. 6, pp. 711–717, 2016.
 26. Han, J., Y. Jun, S. H. Kim, H.-H. Hoang, Y. Jung, S. Kim, J. Kim, R. H. Austin, S. Lee and S. Park, “Rapid Emergence and Mechanisms of Resistance by U87 Glioblastoma Cells to Doxorubicin in an In Vitro Tumor Microfluidic Ecology”, *Proceedings of the National Academy of Sciences*, Vol. 113, No. 50, pp. 14283–14288, 2016.
 27. Gebremicael, G., A. Gebreegziabxier and D. Kassa, “Low Transcriptomic of PTPRCv1 and CD3E is an Independent Predictor of Mortality in HIV and Tuberculosis Co-infected Patient”, *Scientific Reports*, Vol. 12, No. 1, p. 10133, 2022.
 28. Gültekin, Y., *Cloning and Characterization of Novel NOD-Like Receptors as Cytoplasmic Immune Sensors*, M.S. Thesis, Boğaziçi University, 2011.
 29. Yalçinkaya, M., *Characterization of NLRP13 in Inflammasome Activity*, M.S. Thesis, Boğaziçi University, 2015.
 30. Yilmazer, A., *Investigation of NLRP13-Driven Innate Immune Responses*, M.S. Thesis, Boğaziçi University, 2018.
 31. Çıracı, S., *Investigation of NLRP13’s Cleavage and Its Role in Macrophage Polarization*, M.S. Thesis, Boğaziçi University, 2022.
 32. Çakır, E. O., *Investigation of the Role of NLRP13 in Cell Death*, M.S. Thesis, Boğaziçi University, 2022.

33. Duéñez-Guzmán, E. A. and D. Haig, “The Evolution of Reproduction-Related NLRP Genes”, *Journal of Molecular Evolution*, Vol. 78, No. 3-4, pp. 194–201, 2014.

APPENDIX A: PLASMID MAPS

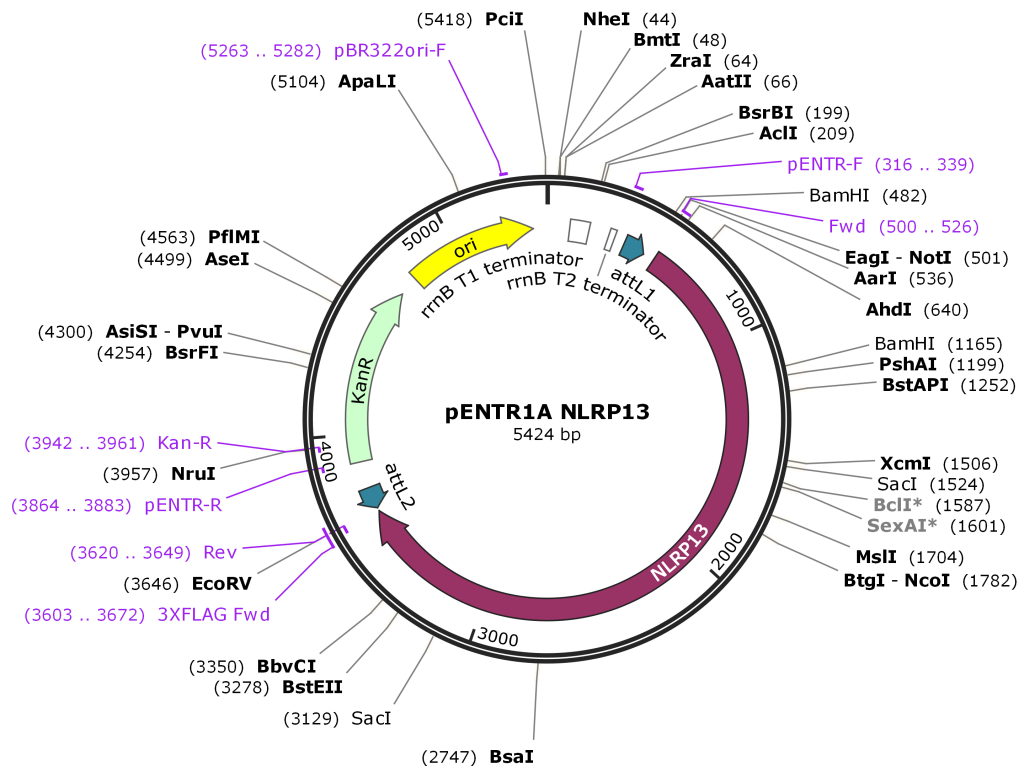


Figure A.1. Map of the pENTR1A-NLRP13 vector.

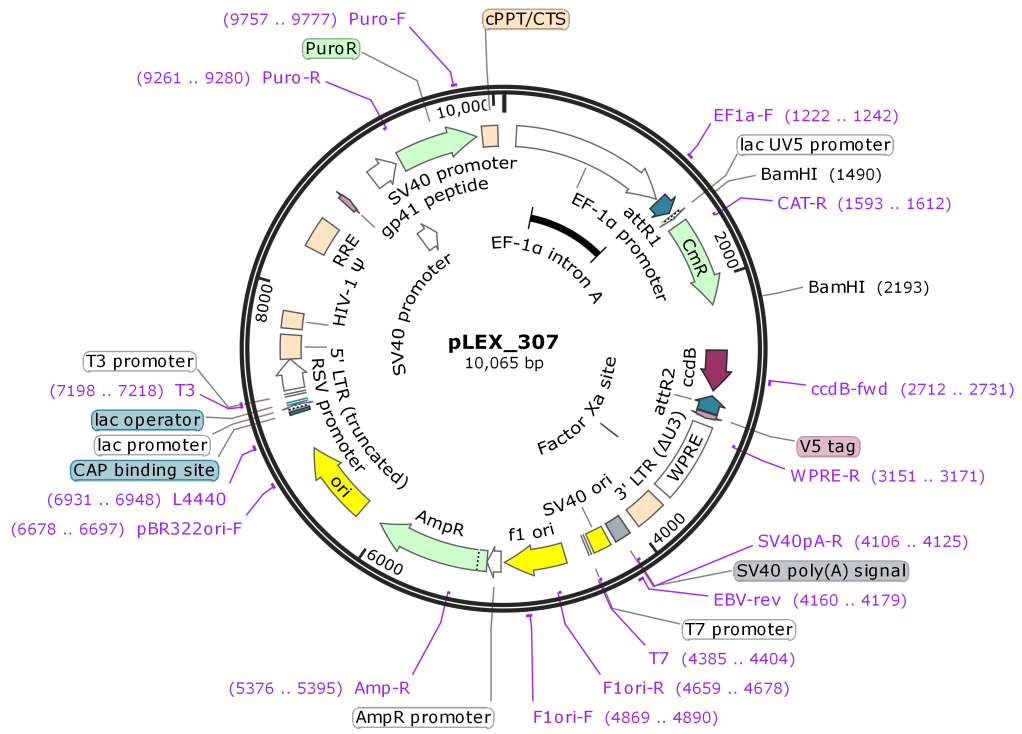


Figure A.2. Map of the pLEX307 cdb vector.